Table of Contents

Materials

4-Vinylbenzoic acid (> 97 %, TCI), 4-ethylbenzoic acid (99 %, Alfa Aesar), copper(II) acetate monohydrate (99.9 %, Alfa Aesar), molybdenum hexacarbonyl (98 %, Sigma-Aldrich), acetic acid-d_3 (99.5 atom % D, Acros Organics) and acetic anhydride-d_6 (99 atom % D, Sigma-Aldrich) were used as received. Styrene (99 %, Merck) was passed through a column of basic alumina (Acros) and stored at -19 °C.

Reactions and characterization methods of all molybdenum compounds were performed under exclusion of moisture and oxygen in flame-dried Schlenk-type glassware or in an argon-filled MBraun glovebox.

Hydrocarbon solvents (THF, *n*-pentane) were dried using an MBraun solvent purification system (SPS-800). THF was additionally distilled under nitrogen from potassium before storage over 4 Å molecular sieves. Prior to use, dimethyl sulfoxide (DMSO) was distilled under nitrogen from CaH_2 and methanol (MeOH) was distilled under nitrogen from magnesium. Dimethyl formamide (DMF) and dichloromethane (DCM) were purchased as analytical grade and used as received.

Deuterated solvents were obtained from Carl Roth GmbH (99.5 atom % D). Prior to use, DMSO-d_6 was distilled from CaH_2 stored and over molecular sieves (4 Å). $CDCl_3$ was distilled, degassed and stored over molecular sieves (4 Å). THF-d_8 was stored over a Na/K alloy.

$[Mo_2(OAc)_4]$[1] and 2,2,6,6-tetramethyl-1-(1-phenylethoxy)piperidine[2] were synthesized according to literature procedures. The deuterated complex $[Mo_2(OAc)_4]$-d_{12} was synthesized according to the procedure for the non-deuterated compound,[1] applying acetic acid-d_3 and acetic anhydride-d_6.

Instrumentation

NMR spectra were recorded on a Bruker Avance 400 (400 MHz) spectrometer. ^1H and $^{13}C\{^1H\}$ NMR chemical shifts were referenced to the residual solvent resonances of $CHCl_3$, DMSO or THF and are reported relative to tetramethylsilane (TMS). ^2H NMR measurements were performed in non-deuterated THF. Abbreviations used in the compounds' analysis include singlet (s), broad singlet (bs), doublet (d), triplet (t), quartet (q) and unresolved multiplet (m). The diffusion coefficients were measured with Diffusion Ordered NMR Spectroscopy (DOSY) experiments, using a Bruker Smart VT unit to control the temperature which was calibrated to be exactly 298 K.

Size-exclusion chromatography (SEC) measurements were performed on a PL-SEC 50 Plus (Polymer Laboratories, Varian), running on tetrahydrofuran (THF) (HPLC-grade). The applied columns were a PLgel Mixed C guard column (50 × 7.5 mm), followed by three PLgel Mixed C linear columns (300 × 7.5 mm, 5µm beadsize) and a differential refractive index (RI) detector. The device was operated at 35 °C column temperature with a flow rate of 1 $mL \cdot min^{-1}$. The columns were calibrated using linear polystyrene standards ranging from 476 to 2.5×10^6 $g \cdot mol^{-1}$. The measured samples were dissolved in THF (2 $mg \cdot mL^{-1}$) and filtered through PTFE membranes with a pore size of 0.2 µm prior to injection. To obtain M_n and $Đ$ values, the integration of the polymer peak was carried out from low elution times to approximately 40 minutes due to overlap with an SEC system peak. No baseline correction was performed. Consequently, M_n and $Đ$ values are estimates.

IR spectra were obtained on a Bruker Tensor 37 FTIR spectrometer, equipped with a room temperature DLaTGS detector and a diamond ATR (attenuated total reflection) unit. Abbreviations used in the compounds' analysis include very strong (vs), strong (s), medium (m), weak (w) and very weak (vw).

Raman spectra were obtained on a Bruker MultiRam spectrometer. Abbreviations used in the compounds' analysis include very strong (vs), strong (s), medium (m), weak (w) and very weak (vw).

Elemental analyses were carried out with an Elementar Micro Cube.

Ultraviolet-visible (UV-Vis) spectra were recorded on a VARIAN Cary 50 Scan UV-Visible Spectrophotometer. Spectra were recorded in THF at room temperature and collected between 200 and 800 nm. Samples were baseline corrected with respect to the pure solvent. For the Cu_2 species a concentration of approx. 0.5 $mg \cdot mL^{-1}$ was applied; for the Mo_2 species a concentration of approx. 0.1 $mg \cdot mL^{-1}$.

Abbreviations

approx.	approximately
ATR	attenuated total reflection
calcd.	calculated
DCM	dichloromethane
DMAc	dimethylacetamide
DMSO	dimethyl sulfoxide
equiv.	equivalents
IR	infra-red
MeOH	methanol
NMR	nuclear magnetic resonance
OAc	acetate
OD	optical density
q. (NMR)	quaternary
RI	refractive index
SCNP	single-chain nanoparticle
SEC	size exclusion chromatography
THF	tetrahydrofuran
UV-Vis	ultraviolet-visible
XRD	X-Ray diffraction

Synthesis

Copolymerization of 4-vinyl-benzoic acid and styrene ($\mathrm{P}_{\mathrm{Acid}}$)

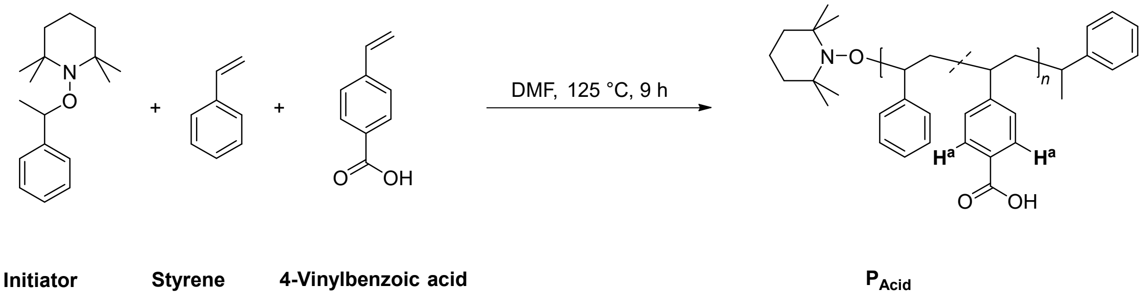

Scheme S1. Nitroxide mediated polymerization of styrene and 4-vinylbenzoic acid, applying the initiator 2,2,6,6-tetramethyl-1-(1-phenylethoxy)piperidine, resulting in copolymer P_{Acid}.

2,2,6,6-Tetramethyl-1-(1-phenylethoxy)piperidine (9.00 mg, 34.4 µmol, 1.00 equiv.) (synthesized according to literature[2]), styrene (2.64 g, 25.3 mmol, 735 equiv.) and 4-vinylbenzoic acid (178 mg, 1.21 mmol, 35.0 equiv.) were dissolved in 1.45 mL of degassed DMF. While stirring, the solution was degassed with N_2 for 30 min. Subsequently, the reaction mixture was heated at 125 °C for 9 h. Cooling to ambient temperature and opening the flask to air, quenched the reaction. After diluting with DCM, the polymer $\mathrm{P}_{\mathrm{Acid}}$ was precipitated twice into cold MeOH, resulting in a white powder. Characterization *via* ^{1}H NMR spectroscopy revealed a monomer ratio of approximately 1:14, regarding the higher amount to styrene (0.65 mmol of benzoic acid functionality in 1.00 g $\mathrm{P}_{\mathrm{Acid}}$).

SEC characterization (THF, RI) resulted in a number average molecular weight of M_n = 32 200 g mol^{-1} and a polydispersity of $Đ$ = 1.2.

^{1}H NMR (400 MHz, THF-d_8): δ [ppm] = 11.2 (bs, COO*H*), 7.91 – 7.51 (m, C*H*-benzoic acid, H^a), 7.25 – 6.27 (m, C*H*-aromatic), 2.59 – 2.83 (m, *H*-backbone).

IR (ATR): $\tilde{\nu}$ [cm^{-1}] = 3082 (vw), 3060 (w), 3026 (s), 3002 (vw), 2923 (s), 2849 (w), 1734 (m), 1690 (m), 1603 (m), 1582 (vw), 1493 (s), 1451 (s), 1423 (w), 1369 (vw), 1315 (vw), 1285 (w), 1179 (w), 1156 (vw), 1086 (vw), 1028 (w), 907 (vw), 856 (vw), 756 (s), 698 (vs), 540 (m).

Raman (solid state): $\tilde{\nu}$ [cm^{-1}] = 3055 (s), 3002 (vw), 2978 (vw), 2903 (m), 2851 (w), 1604 (s), 1584 (m), 1451 (w), 1329 (vw), 1183 (m), 1156 (w), 1032 (m), 1002 (vs), 798 (w), 662 (m), 224 (w).

Cu_2-SCNPs

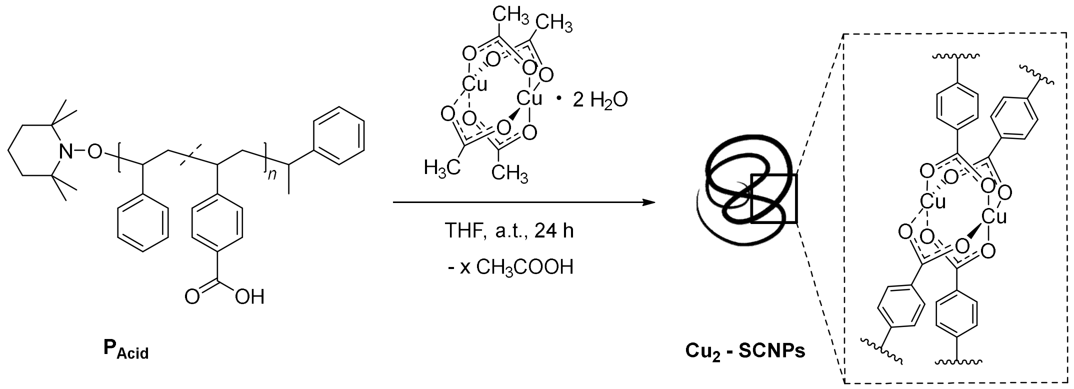

Scheme S2. Intramolecular folding of copolymer ***P_{Acid}****, by addition to a Cu(II) acetate solution, resulting in the formation of* ***Cu_2-SCNPs****. To ensure the collapse into a more compact particle, a carboxylate exchange of at least two acetate ligands is necessary. The depicted folding unit illustrates a replacement of all four acetate ligands by the benzoic acid moieties of* ***P_{Acid}****.*

4.60 mg of copper(II) acetate (11.5 µmol, 0.25 equiv.) was dissolved in 25 mL of THF ($c = 4.6 \cdot 10^{-4}$ mol·L^{-1}). 70.0 mg of copolymer **P_{Acid}** (45.5 µmol benzoic acid functionality, 1.00 equiv.) was dissolved in 100 mL of THF. While stirring the metal-salt solution, the polymer solution was added dropwise with a dropping rate of ~ 5 mL·h^{-1}. After complete addition (20 h), the blue solution was stirred for additional 4 h. The solution was concentrated under reduced pressure and subsequently precipitated into cold MeOH. The solid was filtered off and dried under vacuum, obtaining **Cu_2-SCNPs**.

SEC characterization (THF, RI) resulted in a number average molecular weight of M_n = 24 500 g mol^{-1} and a polydispersity of $Đ$ = 1.2.

^{1}H NMR (400 MHz, THF-d$_8$): δ [ppm] = 7.95 – 7.51 (m, C*H*-benzoic acid), 7.59 – 5.82 (m, C*H*-aromatic), 2.36 – 0.62 (m, *H*-backbone) – The multiplet resonance at δ = 7.95 – 7.51 ppm (C*H*-benzoic acid) is significantly broadened, compared to **P_{Acid}**, due to the coordination of paramagnetic Cu(II) ions. At δ = 11.2 ppm a singlet resonance is detected for R-COO*H*, indicating free carboxylic acid moieties, most likely due to an axial coordination of the acidic functionalities to the Cu_2^{4+} moieties.

IR (ATR): $\tilde{\nu}$ [cm^{-1}] = 3083 (vw), 3060 (w), 3026 (s), 3001 (vw), 2923 (s), 2849 (w), 1733 (w), 1691 (w), 1619 (m), 1603 (m), 1583 (vw), 1565 (vw), 1493 (s), 1452 (s), 1407 (s), 1374 (vw), 1181 (w), 1155 (vw), 1070 (vw), 1028 (w), 907 (w), 857 (vw), 757 (s), 698 (vs), 540 (m).

Mo_2-SCNPs

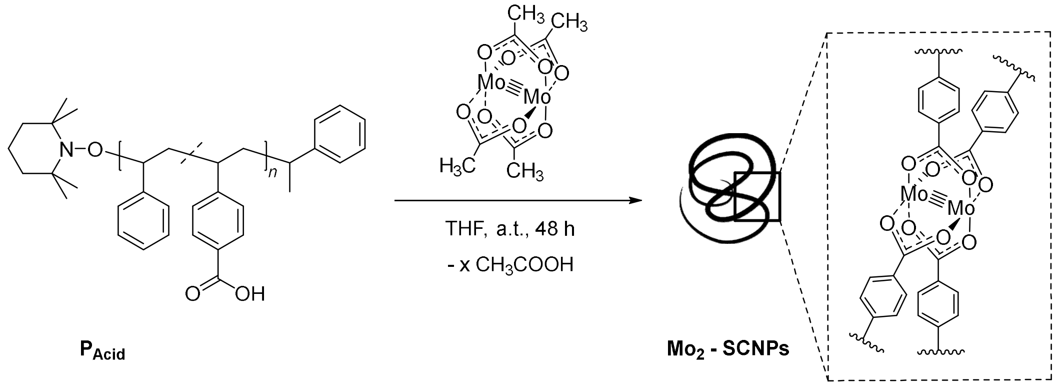

Scheme S3. Intramolecular folding of copolymer ***P_{Acid}****, by addition to a Mo(II) acetate solution, resulting in the formation of* ***Mo_2-SCNPs****. To ensure the collapse into a more compact structure, a carboxylate exchange of at least two acetate ligands is necessary. The depicted folding unit illustrates a replacement of all four acetate ligands by the benzoic acid moieties of* ***P_{Acid}****.*

For the synthesis of **Mo_2-SCNPs** the exclusion of water and oxygen is essential. Therefore, Schlenk techniques were applied and only dry and degassed solvents (THF, MeOH) were used.

7.00 mg of molybdenum(II) acetate (16.3 µmol, 0.25 equiv.) was dissolved in 50 mL of THF ($c = 3.3 \cdot 10^{-4}$ mol·L^{-1}). 100 mg of copolymer **P_{Acid}** (65.0 µmol benzoic acid functionality, 1.00 equiv.) was dissolved in 120 mL of THF. While stirring the metal salt solution, the polymer solution was added dropwise with a dropping rate of ~ 3 mL·h^{-1}. After complete addition (40 h), the yellow solution was stirred for additional 8 h. The solution was concentrated under reduced pressure and subsequently precipitated into cold MeOH. The solid was filtered off and dried under vacuum, yielding **Mo_2-SCNPs**.

For analytical purposes an analogous procedure was performed, applying the deuterated complex $[Mo_2(OAc)_4]$-d_{12} to obtain **Mo_2-SCNPs** (refer to Figures S12 and S13).

SEC analysis was not feasible, as **Mo_2-SCNPs** are highly air and moisture sensitive.

^{1}H NMR (400 MHz, $CDCl_3$): δ [ppm] = 8.16 – 7.54 (m, C*H*-benzoic acid), 7.37 – 6.13 (m, C*H*-aromatic), 2.55 – 0.89 (m, *H*-backbone). – Additional NMR measurements in THF-d_8 revealed no free carboxylic acid proton resonances (Figure S9).

Raman (solid state): $\tilde{\nu}$ [cm^{-1}] = 3055 (s), 3000 (vw), 2977 (vw), 2910 (m), 2851 (w), 1606 (s), 1583 (m), 1513 (m), 1451 (w), 1411 (s), 1401 (s), 1332 (vw), 1184 (m), 1156 (w), 1032 (m), 1002 (vs), 795 (w), 622 (m), 408 (w), 225 (w).

IR (ATR): $\tilde{\nu}$ [cm^{-1}] = 3082 (vw), 3060 (w), 3026 (s), 3001 (vw), 2922 (s), 2849 (w), 1602 (m), 1556 (w), 1493 (s), 1451 (s), 1401 (m), 1181 (w), 1154 (vw), 1068 (vw), 1028 (w), 907 (w), 845 (vw), 756 (s), 698 (vs), 540 (m).

UV-Vis: $\lambda_{max.}$ [nm] = 433.

Model Complexes

General Information

The synthesis of the compounds 1 and 2 in THF or DMSO leads to an axial solvent coordination to the M_2^{4+} unit, which cannot always be removed in vacuum. Thus, residues of THF and DMSO can be observed in the corresponding NMR-, IR- and Raman spectra as well as elemental analysis.

$[Cu_2(p\text{-}O_2CPhEt)_4] \cdot 2$ dmso (1):

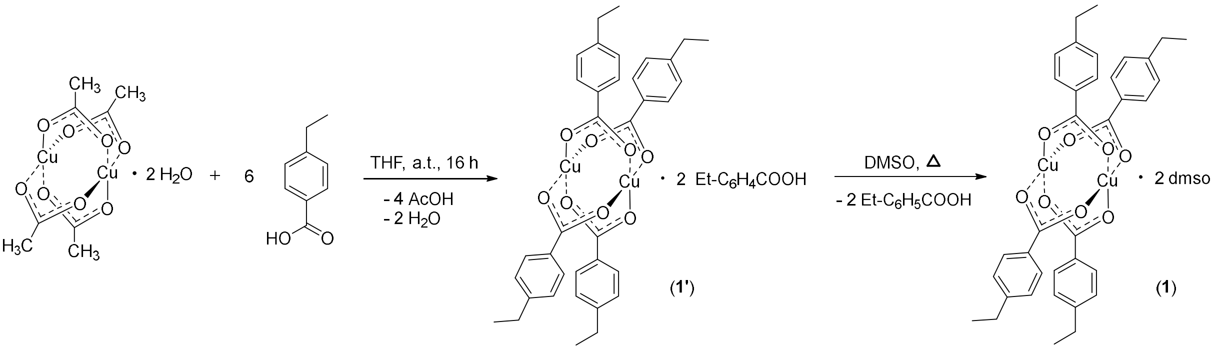

Scheme S4. Synthesis of the Cu_2-complex 1′ via a carboxylic exchange reaction in THF. In addition to the four bridging carboxylates, two additional carboxylic acids coordinate axially to the Cu_2^{4+} unit. Subsequent crystallization from hot DMSO leads to an axial ligand replacement (Cu_2-model complex 1).

The di-copper complex $[Cu_2(p\text{-}O_2CPhEt)_4(p\text{-}HO_2CPhEt)_2]$ (1′) was synthesized according to literature procedure,[3] reacting copper(II) acetate (300 mg, 0.75 mmol, 1.00 equiv.) with 4-ethylbenzoic acid (733 mg, 4.88 mmol, 6.50 equiv.) in THF. Subsequent crystallization from DMSO led to the substitution of both axially binding 4-ethyl benzoic acid moieties by two solvent molecules of DMSO (refer to Figure S1). Crystalline yield (1): 500 mg (76 %).

IR (ATR): $\tilde{\nu}$ [cm^{-1}] = 2962 (m), 2928 (vw), 2868 (vw), 1619 (s), 1564 (m), 1455 (vw), 1398 (vs), 1308 (w), 1177 (m), 1113 (vw), 1057 (m), 1019 (s), 956 (w), 933 (vw), 861 (w), 850 (w), 785 (m), 766 (m), 710 (m), 628 (m), 533 (vw), 457 (w).

Anal Calcd. (%) for $[C_{36}H_{36}Cu_2O_8 \cdot 4\ C_2H_6SO]$ (1036.28 g·mol^{-1}): C 51.00, H 5.84, S 12.37; found C 51.69, H 6.00, S 12.39.

No meaningful NMR analysis was feasible due to the paramagnetic Cu_2^{4+} moiety.

$[Mo_2(p\text{-}O_2CPhEt)_4] \cdot 2$ dmso (2):

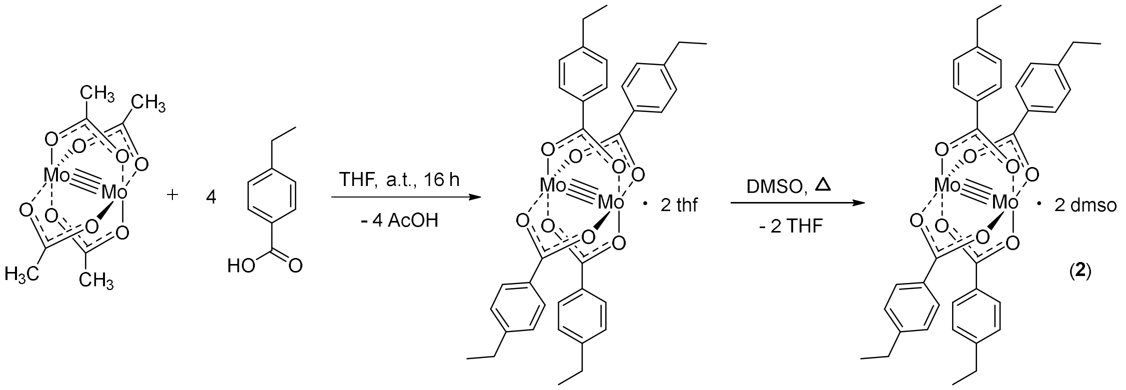

Scheme S5. Synthesis of the Mo_2-model complex ***2*** *via a carboxylic exchange reaction and subsequent crystallization from hot DMSO.*

Molybdenum(II) acetate (300 mg, 0.70 mmol, 1.00 equiv.) and 4-ethylbenzoic acid (474 mg, 3.15 mmol, 4.50 equiv.) were dissolved in THF (20 mL) and stirred at room temperature for 24 h. The solution was concentrated under reduced pressure. After addition of *n*-pentane (20 mL) an orange solid precipitated, which was filtered off and dried under reduced pressure. Single crystals, suitable for X-ray analysis, were obtained after slow cooling of a hot DMSO solution (refer to Figure S3), leading to an axial DMSO coordination. Crystalline yield: 430 mg (78 %).

^{1}H NMR (400 MHz, DMSO-d$_6$): δ [ppm] = 8.09 (d, $^3J_{H,H}$ = 8.3 Hz, 8H, Ph), 7.36 (d, $^3J_{H,H}$ = 8.3 Hz, 8H, Ph), 2.67 (q, $^3J_{H,H}$ = 7.5 Hz, 8H, CH_2), 1.17 (t, $^3J_{H,H}$ = 7.6 Hz, 12H, CH_3). – An additional resonance (s) for residually coordinated DMSO is observed at δ = 2.54 ppm.

^{13}C{^{1}H} NMR (101 MHz, DMSO-d$_6$): δ [ppm] = 175.6 (RCO_2), 148.1 (Ph, $C_{q.}$), 129.8 (Ph), 128.5 (Ph, $C_{q.}$), 128.1 (Ph), 28.1 (CH_2), 15.4 (CH_3).

IR (ATR): $\tilde{\nu}$ [cm^{-1}] = 2961 (m), 2928 (w), 2867 (vw), 1606 (w), 1578 (w), 1488 (s), 1460 (s), 1394 (vs), 1304 (w), 1178 (m), 1139 (vw), 1110 (vw), 1060 (m), 1017 (s), 953 (vw), 849 (s), 765 (s), 707 (m), 624 (m), 527 (m), 457 (m), 412 (vw).

Raman (solid state): $\tilde{\nu}$ [cm^{-1}] = 1608 (s), 1515 (s), 1414 (vs), 1398 (vs), 1205 (vw), 1182 (w), 1061 (vw), 1022 (vw), 864 (vw), 771 (w), 638 (m), 532 (vw), 465 (m), 453 (m), 403 (m), 372 (w), 157 (m).

Anal Calcd. (%) for $[C_{36}H_{36}Mo_2O_8 \cdot C_2H_6SO]$ (866.73 g·mol^{-1}): C 52.66, H 4.88, S 3.70; found C 51.18, H 4.98, S 3.59.

UV-Vis: $\lambda_{max.}$ [nm] = 432.

Single-Crystal X-Ray Diffraction (XRD)

A suitable crystal was covered in mineral oil (Aldrich) and mounted on a glass fiber. The crystal was transferred directly to the cold stream of a STOE IPDS 2 or a STOE StadiVari diffractometer. All structures were solved by using the program SHELXS/T[4-5] and Olex2.[6] The remaining non-hydrogen atoms were located from successive difference Fourier map calculations. The refinements were carried out by using full-matrix least-squares techniques on F^2 by using the program SHELXL.[4-5] In each case, the locations of the largest peaks in the final difference Fourier map calculations, as well as the magnitude of the residual electron densities, were of no chemical significance.

Crystallographic data (excluding structure factors) for the structures reported in this paper have been deposited with the Cambridge Crystallographic Data Centre as a supplementary publication no. 1873610-1873611. Copies of the data can be obtained free of charge on application to CCDC, 12 Union Road, Cambridge CB21EZ, UK (fax: (+(44)1223-336-033; email: deposit@ccdc.cam.ac.uk).

Refinement Details:

The crystal structure of compound 2 contains one molecule of coordinating and one of non-coordinating DMSO in the asymmetric unit. The solvent molecules are disordered and therefore were split and modeled accordingly.

Table S1. Crystal data and structure refinement of compounds 1 *and* 2.

Compound	**1**	**Compound**	**2**
Formula	$C_{44}H_{60}Cu_2O_{12}S_4$	Formula	$C_{44}H_{36}D_{24}Mo_2O_{12}S_4$
D_{calc}/g·cm^{-3}	1.391	D_{calc}/g·cm^{-3}	1.482
μ/mm^{-1}	1.085	μ/mm^{-1}	0.719
Formula Weight/g·mol^{-1}	1036.24	Formula Weight/g·mol^{-1}	1125.18
Colour	blue	Colour	red
Shape	rod	Shape	fragment
Size/mm^3	0.37×0.17×0.06	Size/mm^3	0.51×0.43×0.35
T/K	100	T/K	210(2)
Crystal System	orthorhombic	Crystal System	triclinic
Space Group	$Pna2_1$	Space Group	P-1
a/Å	14.0648(4)	a/Å	10.066(2)
b/Å	22.4851(5)	b/Å	11.500(2)
c/Å	15.6445(3)	c/Å	12.806(3)
		α/°	67.91(3)
		β/°	88.31(3)
		γ/°	67.80(3)
V/Å^3	4947.5(2)	V/Å^3	1260.7(6)
Z	4	Z	1
Wavelength/Å	0.71073	Wavelength/Å	0.71073
Radiation type	MoK$_\alpha$	Radiation type	MoK$_\alpha$
Θ_{min}/°	1.586	Θ_{min}/°	1.731
Θ_{max}/°	30.312	Θ_{max}/°	26.116
Measured Refl.	59169	Measured Refl.	9552
Independent Refl.	13111	Independent Refl.	4916
Reflections with I > 2(I)	10628	Reflections with I > 2(I)	4214
R_{int}	0.0564	R_{int}	0.0163
Parameters	571	Parameters	353
Restraints	1	Restraints	0
Largest Peak	1.616	Largest Peak	0.614
Deepest Hole	-0.957	Deepest Hole	-0.257
GooF	1.021	GooF	0.965
wR_2 (all data)	0.1256	wR_2 (all data)	0.0642
wR_2	0.1164	wR_2	0.0632
R_1 (all data)	0.0712	R_1 (all data)	0.0311
R_1	0.0509	R_1	0.0257
Flack Parameter	-0.024(8)		
Hooft Parameter	-0.012(4)		

Solid State Structures

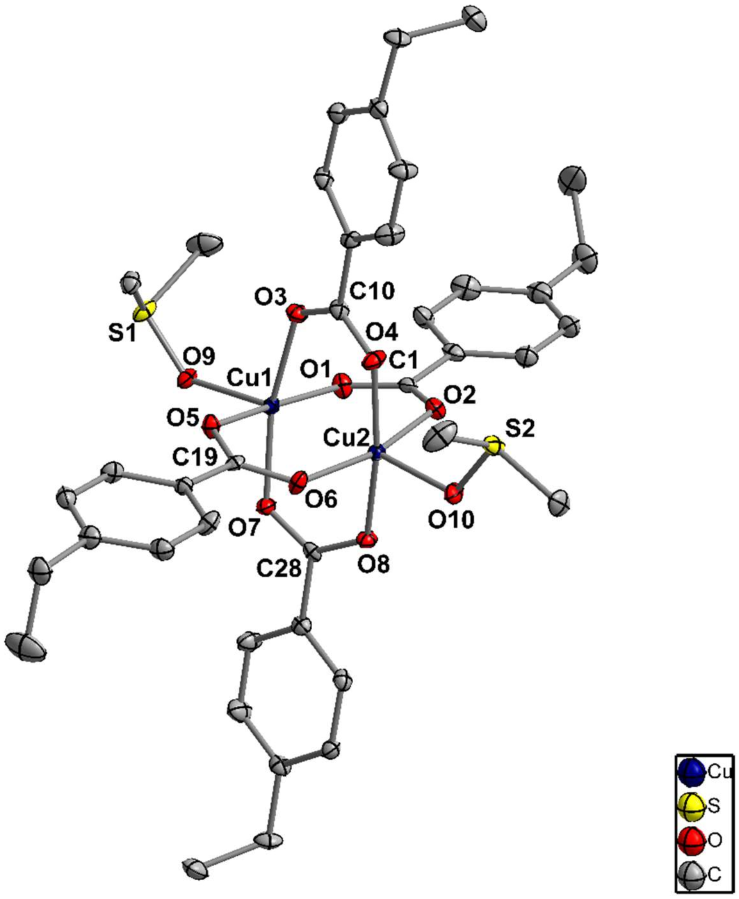

Figure S1. Molecular structure of compound **1** *in the solid state, displayed with an ellipsoid probability of 50 %. Hydrogen atoms and non-coordinating solvent molecules (two molecules of DMSO per asymmetric unit) are omitted for clarity. Selected bond lengths [Å] and angles [°]: Cu1-Cu2 2.6021(8), Cu1-O1 1.942(4), Cu1-O3 2.008(4), Cu1-O5 1.941(4), Cu1-O7 1.991(3), Cu1-O9 2.130(4), Cu2-O2 2.005(3), Cu2-O4 1.954(4), Cu2-O6 1.991(4), Cu2-O8 1.934(3), Cu2-O10 2.108(4), S1-O9 1.510(4), S2-O10 1.510(4), O1-C1 1.264(6), O2-C1 1.258(6), O3-C10 1.262(6), O4-C10 1.251(6), O5-C19 1.265(6), O6-C19 1.265(6), O7-C28 1.266(6), O8-C28 1.270(6). O1-Cu1-Cu2 84.78(11), O1-Cu1-O3 87.3(2), O1-Cu1-O7 91.1(2), O3-Cu1-Cu2 83.10(10), O5-Cu1-Cu2 87.74(11), O5-Cu1-O1 172.1(2), O5-Cu1-O3 89.2(2), O5-Cu1-O7 90.3(2), O7-Cu1-Cu2 82.70(10), O7-Cu1-O3 165.8(2), O9-Cu1-Cu2 173.21(10), O2-Cu2-Cu1 84.04(10), O4-Cu2-Cu1 85.45(11), O4-Cu2-O2 88.2(2), O4-Cu2-O6 88.4(2), O6-Cu2-Cu1 81.09(10), O6-Cu2-O2 164.97(14), O8-Cu2-Cu1 86.29(10), O8-Cu2-Cu1 86.29(10), O8-Cu2-O2 92.1(2), O8-Cu2-O4 171.6(2), O8-Cu2-O6 89.0(2), O10-Cu2-Cu1 173.70(11), O2-C1-O1 125.6(5), O4-C10-O3 125.7(5), O6-C19-O5 124.9(5), O7-C28-O8 124.7(4).*

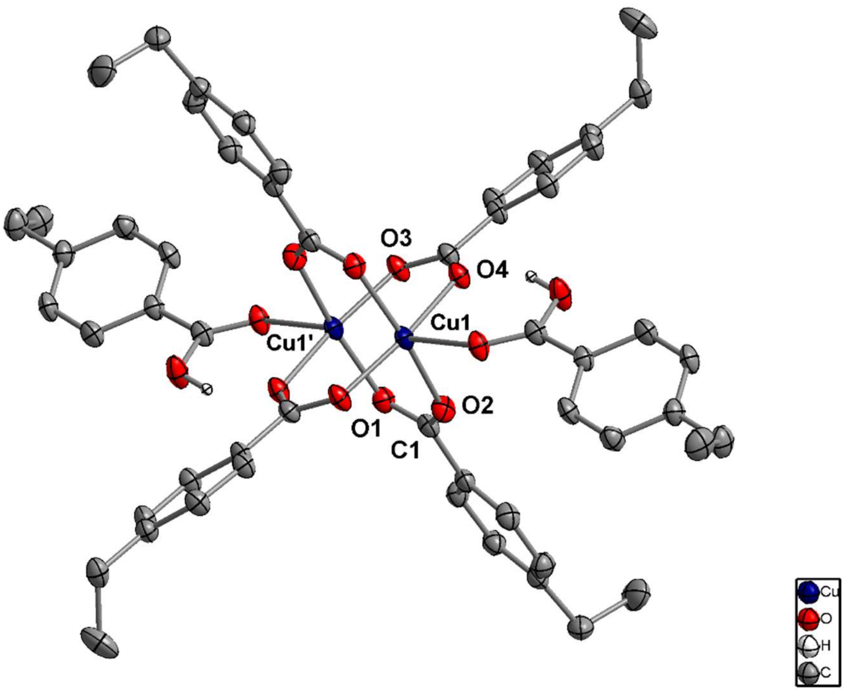

*Figure S2. Molecular structure of compound **1'** in the solid state, displayed with an ellipsoid probability of 30 %. Most of the hydrogen atoms are omitted for clarity. This solid state structure has been reported in literature before.*[3]

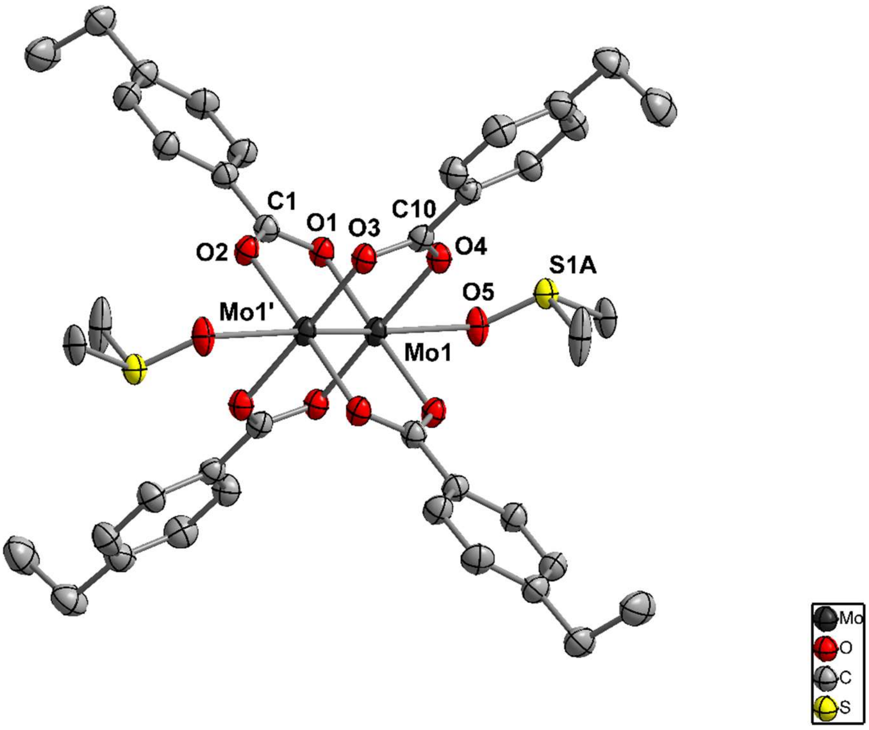

*Figure S3. Molecular structure of compound **2** in the solid state, displayed with an ellipsoid probability of 30 %. Hydrogen atoms and non-coordinating solvent molecules (one molecule of DMSO per asymmetric unit) are omitted for clarity. Selected bond lengths [Å] and angles [°]: Mo1-Mo1' 2.1153(5), Mo1-O1 2.106(2), Mo1'-O2 2.120(2), Mo1'-O3 2.111(2), Mo1-O4 2.125(2), Mo1-O5 2.4924(14), O1-C1 1.280(2), O2-C1 1.277(2), O3-C10 1.279(2), O4-C10 1.278(2), O5-S1A 1.501(2). Mo1-Mo1'-O2 90.68(5), Mo1'-Mo1-O4 90.24(5), Mo1'-Mo1-O5 168.27(4), O1-Mo1-Mo1' 92.52(5), O1-Mo1-O4 91.26(7), O1-Mo1-O5 93.40(6), O3-Mo1'-Mo1 92.96(5), O3-Mo1'-O2 91.38(7), O4-Mo1-O5 79.52(6), O2-C1-O1 121.6(2), O4-C10-O3 121.7(2).*

Original Data

NMR spectra

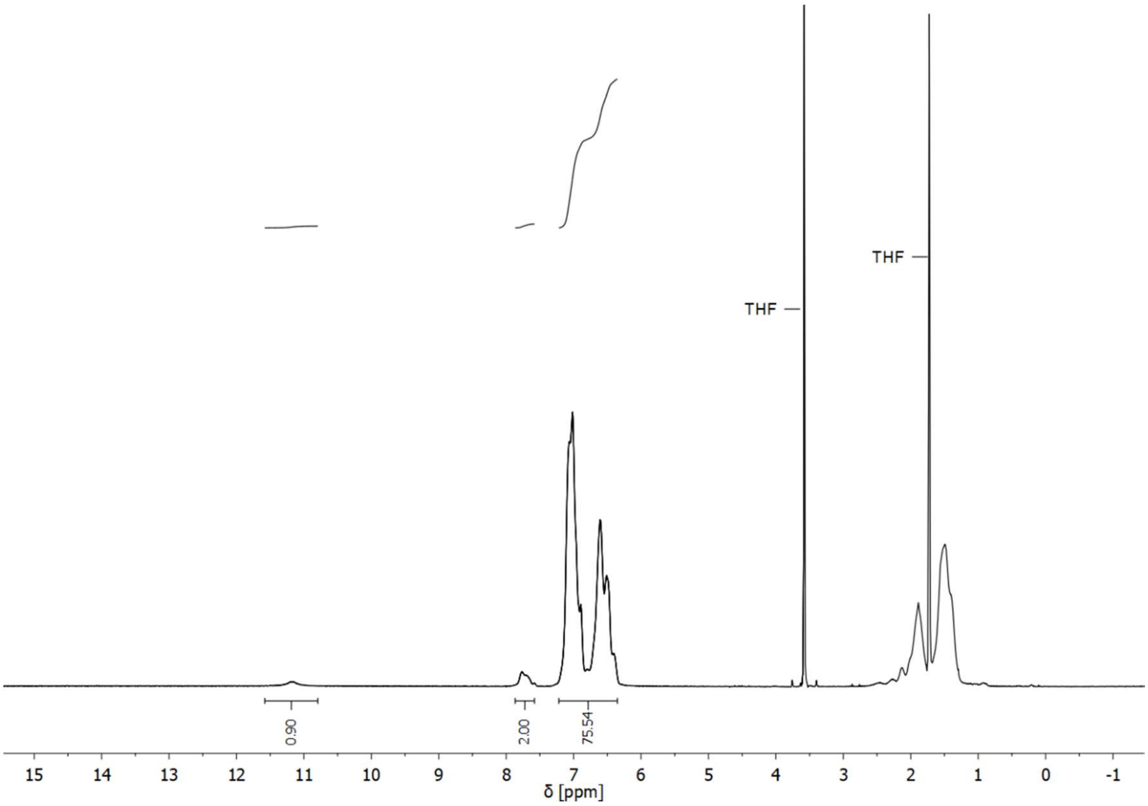

Figure S4. *^{1}H NMR spectrum of **P_{Acid}** in THF-d_8 (400 MHz; 298 K).*

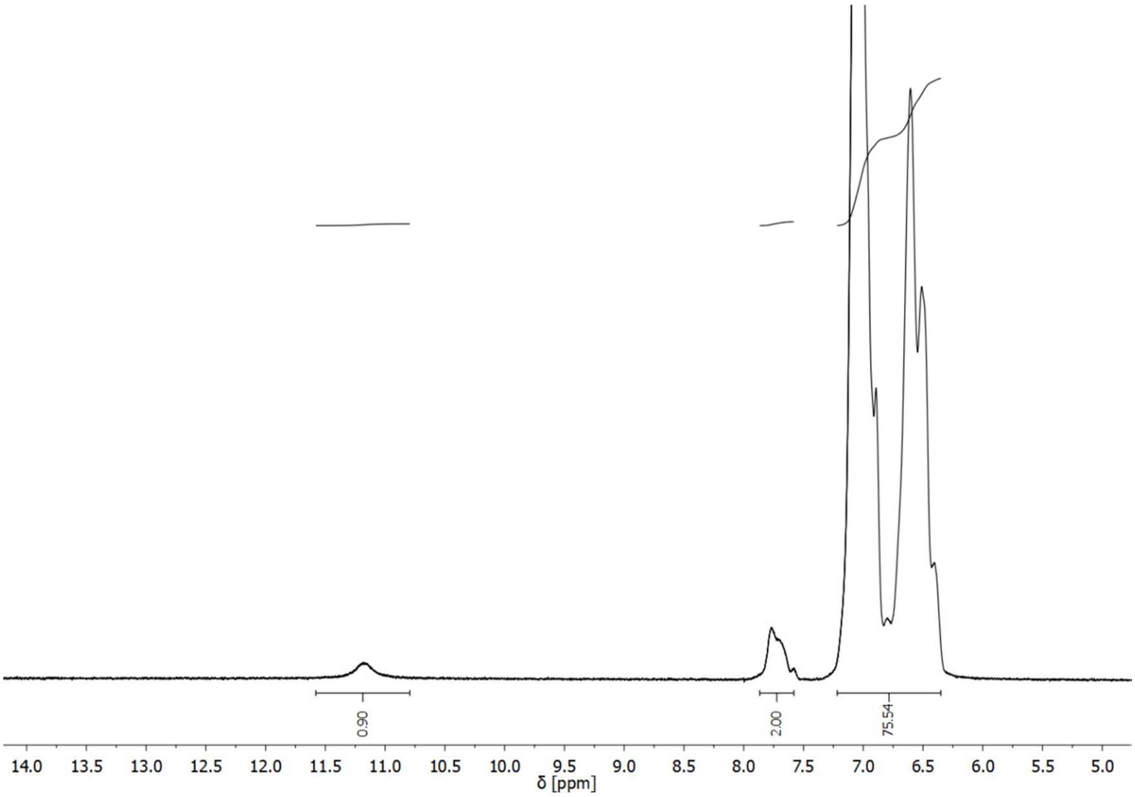

Figure S5. *Magnified excerpt of Figure S4 (^{1}H NMR, **P_{Acid}** in THF-d_8), depicting the acidic proton resonance at δ = 11.2 ppm .*

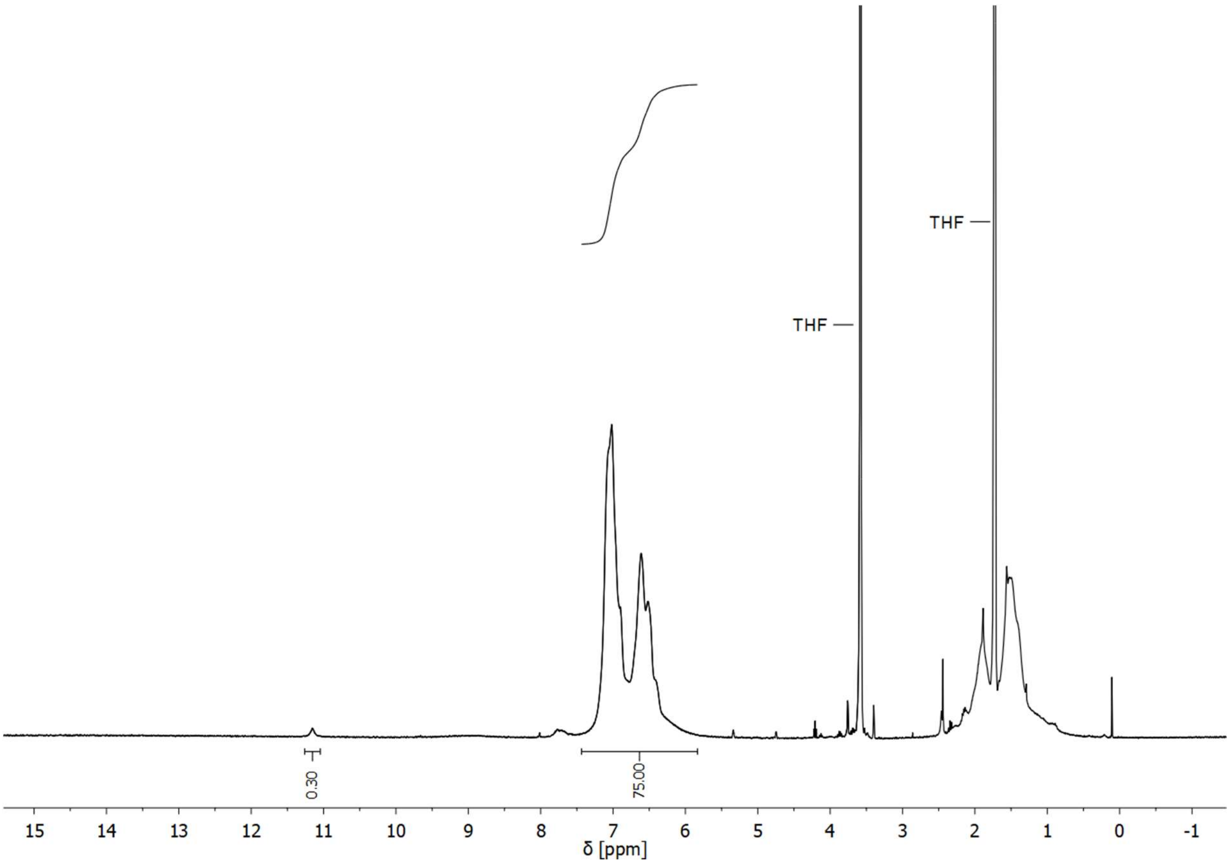

Figure S6. ^{1}H NMR spectrum of **Cu$_2$-SCNPs** in THF-d_8 (400 MHz; 298 K). In comparison to **P$_{Acid}$** (Figure S4), about a third of the acidic proton resonances is detected. The presence of free carboxylic acid moieties is most likely due to an axial coordination of the acidic functionalities to the Cu$_2^{4+}$ moieties (refer to Figure S2, solid state structure).

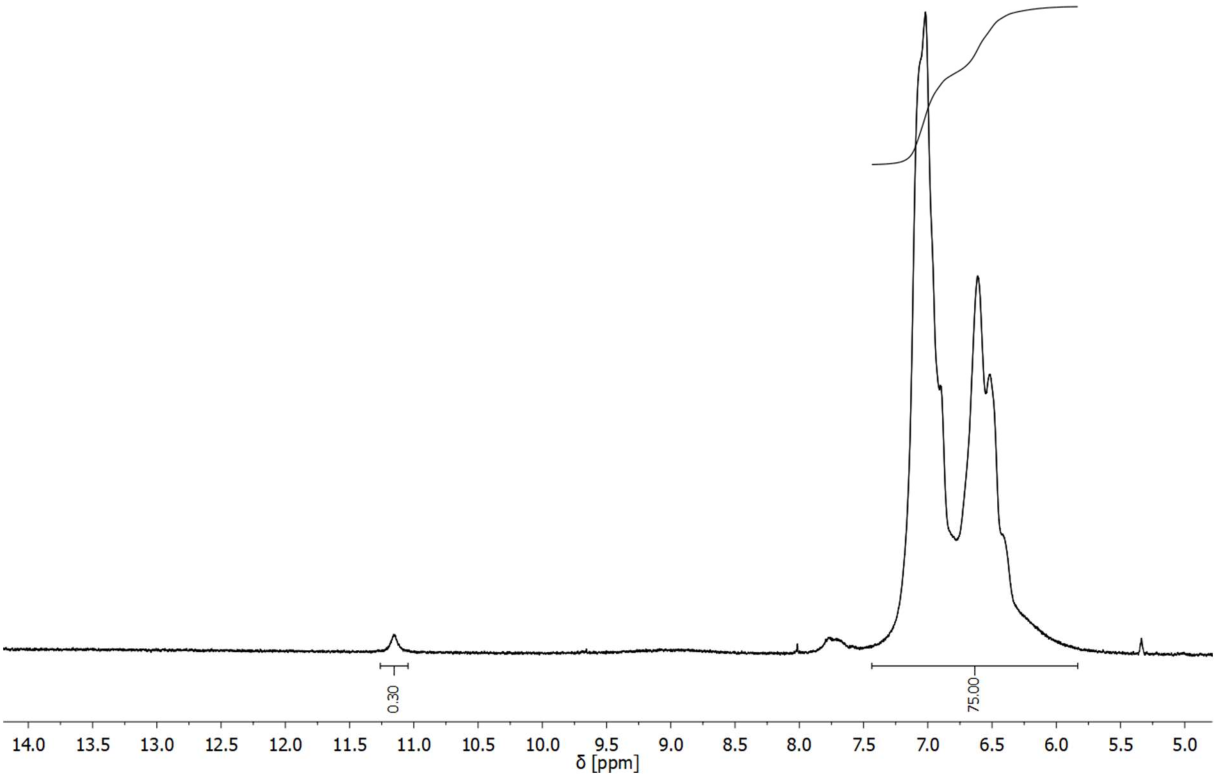

Figure S7. Magnified excerpt of Figure S6 (^{1}H NMR, **Cu$_2$-SCNPs** in THF-d_8).

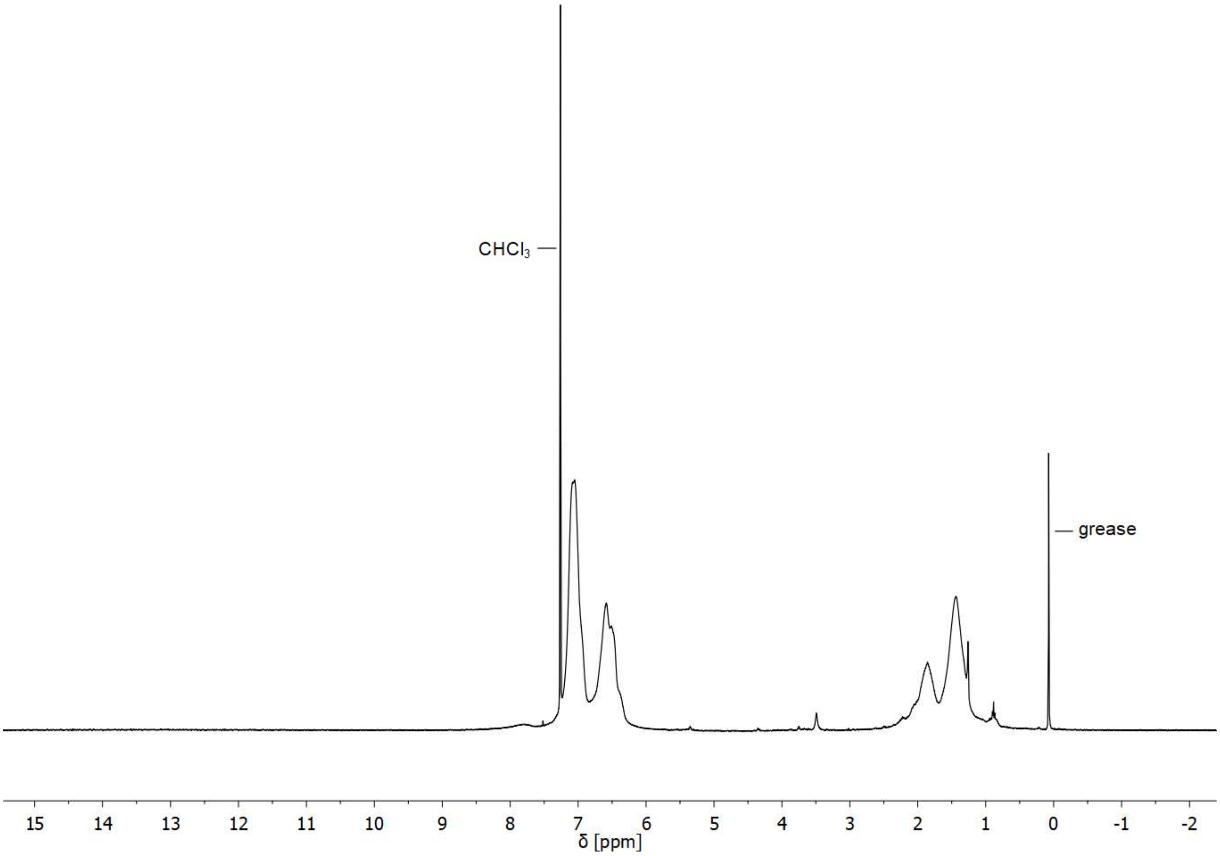

Figure S8. ^{1}H NMR spectrum of **Mo$_2$-SCNPs** in CDCl$_3$ (400 MHz; 298 K).

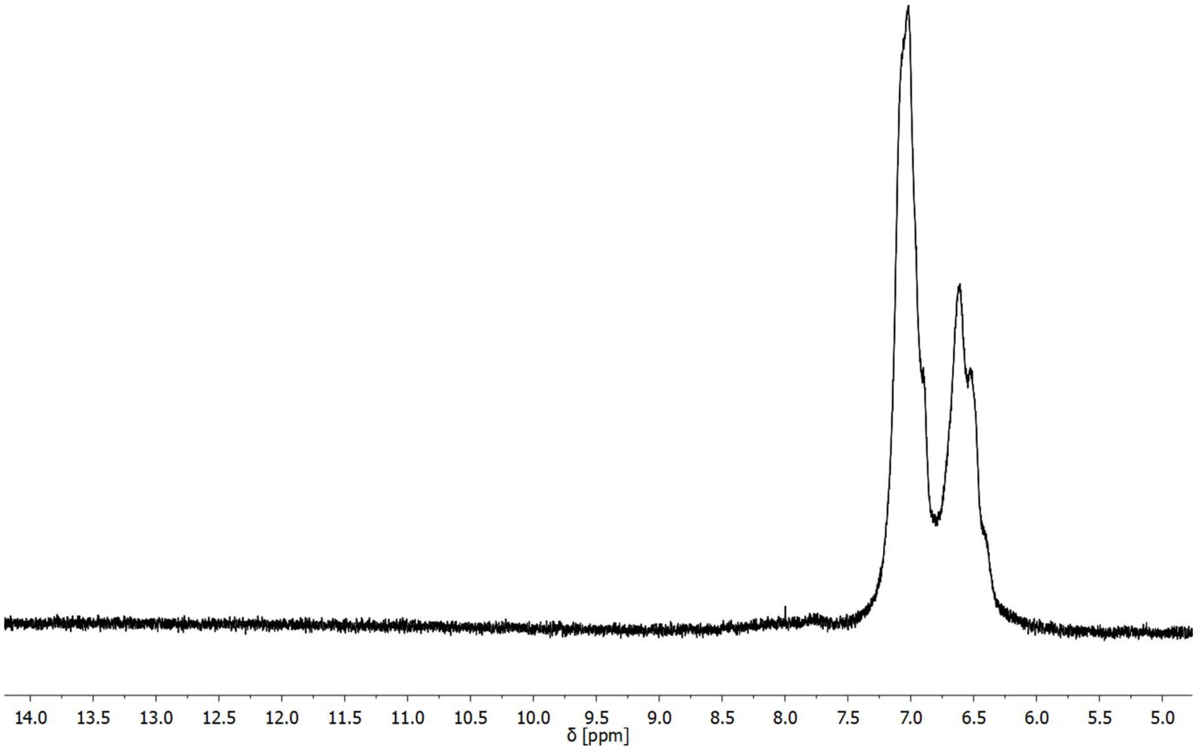

Figure S9. *Magnified excerpt of ^{1}H NMR spectrum of* ***Mo$_2$-SCNPs*** *in THF-d$_8$ (400 MHz; 298 K). In contrary to the* ***Cu$_2$-SCNPs*** *(Figure S6 and S7), no resonances for the carboxylic acid moieties are detected in the downfield area.*

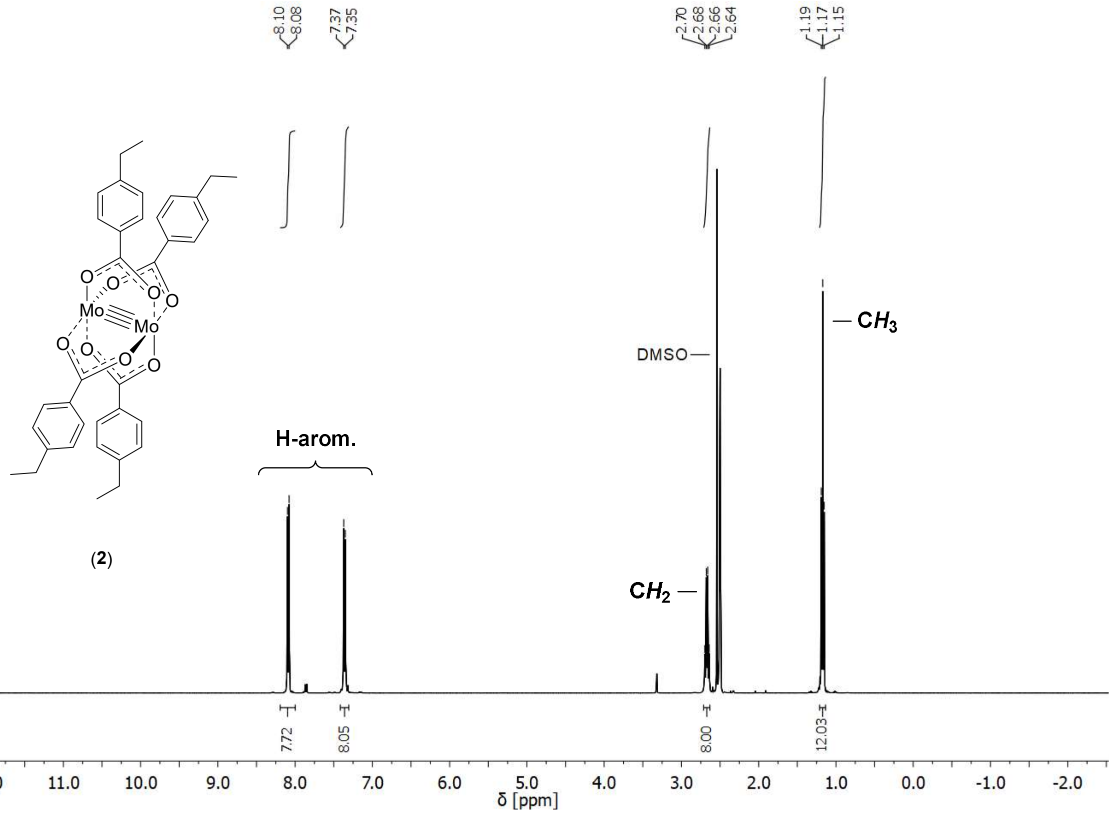

Figure S10. ^1H *NMR spectrum of* Mo_2*-model complex* ***2*** *in DMSO-*d_6 *(400 MHz; 298 K).*

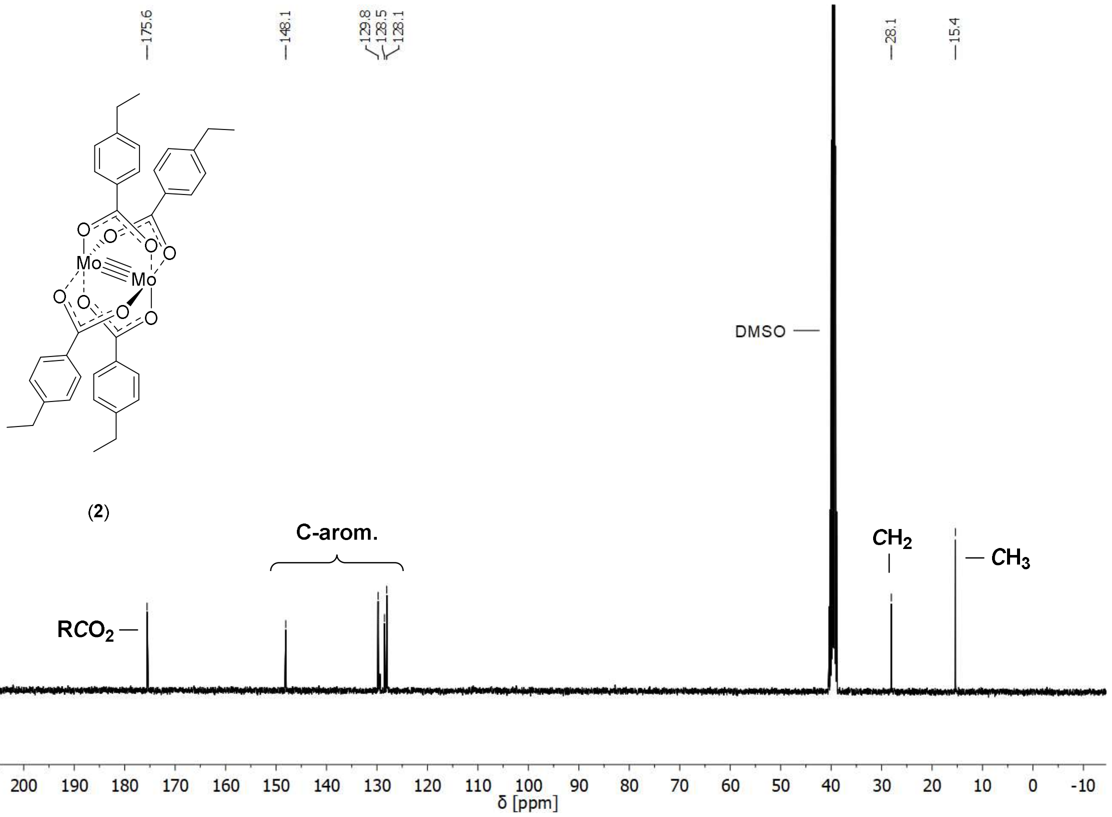

Figure S11. $^{13}C\{^1H\}$ *NMR spectrum of* Mo_2*-model complex* ***2*** *in DMSO-*d_6 *(101 MHz; 298 K).*

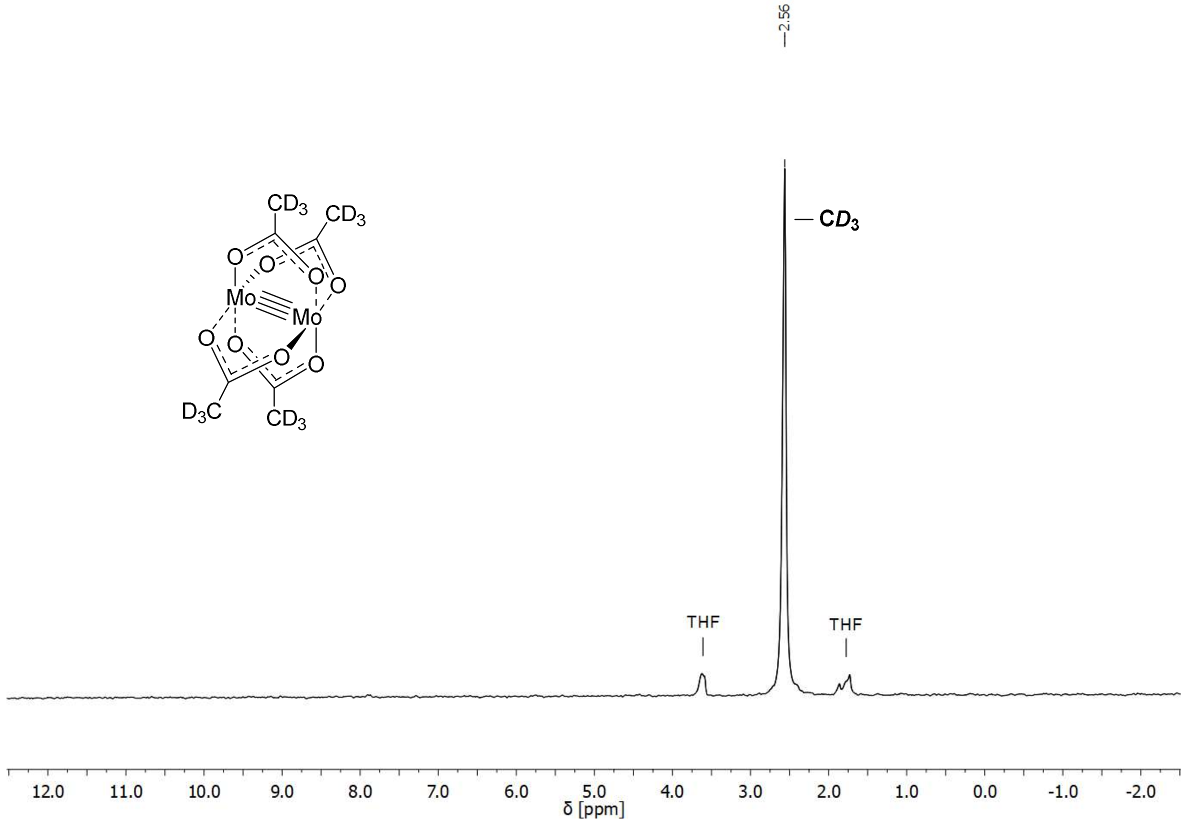

Figure S12. ^{2}H NMR spectrum of $[Mo_2(OAc)_4]$-d_{12} in THF (61 MHz; 298 K).

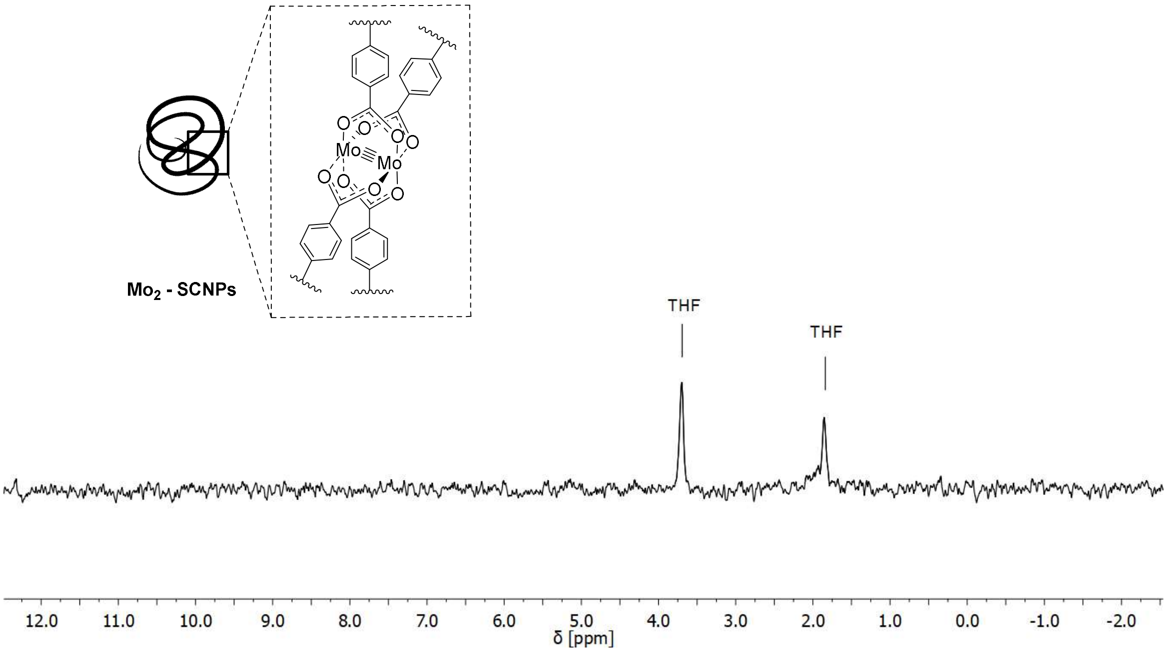

Figure S13. ^{2}H NMR spectrum of ***Mo$_2$-SCNPs*** (applying $[Mo_2(OAc)_4]$-d_{12}) in THF (61 MHz; 298 K). The absence of any -CD_3 resonances (compare to Figure S12) indicates a complete substitution of the deuterated acetate ligands by the benzoic acid moieties of ***P_{Acid}***.

DOSY Measurements

Molecules are distinguished according to their diffusion coefficient, which correlates with their hydrodynamic radius (*R_o*). Copolymer $\mathrm{P_{Acid}}$, $\mathrm{Cu_2}$-SCNPs and $\mathrm{Mo_2}$-SCNPs were analysed in $\mathrm{CDCl_3}$ (*c* ~ 12 mg·mL^{-1}), employing a dynamic viscosity of η = 0.0005418 $\frac{N}{m^2}s$ (at 298.15 K).[7] Calculation of the hydrodynamic radius was carried out, applying the Stokes-Einstein Equation.

$$Stokes - Einstein\ Equation: \qquad D = \frac{k_B \cdot T}{6\pi \cdot \eta \cdot R_0} \ ; \quad R_0 = \frac{k_B \cdot T}{6\pi \cdot \eta \cdot \mathrm{D}}$$

$$k_B = 1.38 \cdot \frac{10^{-23} J}{K}; \qquad T = 298.15\,K\,; \quad \eta(DMSO) = 0.5418\,cP = 0.5418\,mPa \cdot s\ (at\ 298.15\,K)$$

$$1\,Pa = 1\frac{N}{m^2}\ ; \quad 1\,J = 1\,N \cdot m$$

$$R_0 = \frac{1.38 \cdot 10^{-23}\frac{J}{K} \cdot 298.15\,K}{6\pi \cdot 0.0005418\frac{N}{m^2}s} \cdot \frac{1}{D}$$

$$R_0 = \frac{4.115 \cdot 10^{-21} Jm^2}{0.0102127\,\mathrm{Ns}} \cdot \frac{1}{D}$$

$$R_0 = 4.029 \cdot 10^{-19}\frac{m^3}{s} \cdot \frac{1}{D}$$

$\mathrm{P_{Acid}}$: $D_{av.} = 1.03 \ \cdot 10^{-10}\frac{m^2}{s};\ (averaged\ six\ values)$

$R_0 = 3.91 \cdot 10^{-9}\,m = 3.91\,\mathrm{nm}$

$\mathrm{Cu_2}$-SCNPs: $D_{av.} = 1.77 \ \cdot 10^{-10}\frac{m^2}{s};\ (averaged\ five\ values)$

$R_0 = 2.28 \cdot 10^{-9}\,m = 2.28\,\mathrm{nm}$

$\mathrm{Mo_2}$-SCNPs: $D_{av.} = 1.57 \ \cdot 10^{-10}\frac{m^2}{s};\ (averaged\ five\ values)$

$R_0 = 2.57 \cdot 10^{-9}\,m = 2.57\,\mathrm{nm}$

DOSY report P_{Acid}:

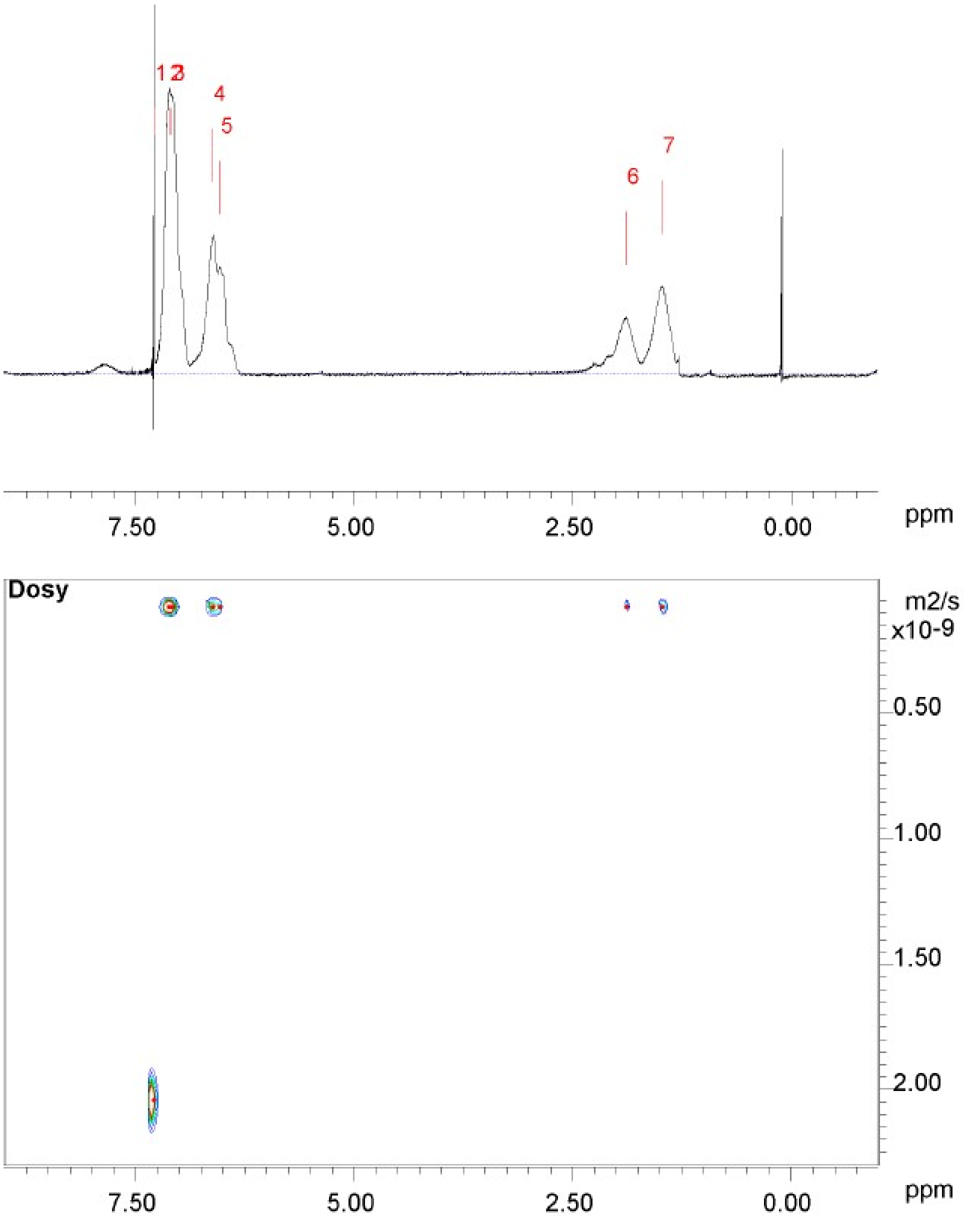

Peak name	F2 [ppm]	D [m2/s]	error
1	7.285	2.09e-09	5.450e-11
2	7.112	1.01e-10	5.247e-12
3	7.080	1.03e-10	4.816e-12
4	6.614	9.97e-11	5.524e-12
5	6.534	1.05e-10	5.020e-12
6	1.881	1.03e-10	6.629e-12
7	1.466	1.05e-10	5.025e-12

Figure S14. *DOSY report of P_{Acid}; measured in $CDCl_3$ (peak 1) at 298 K.*

DOSY report **Cu$_2$-SCNPs**:

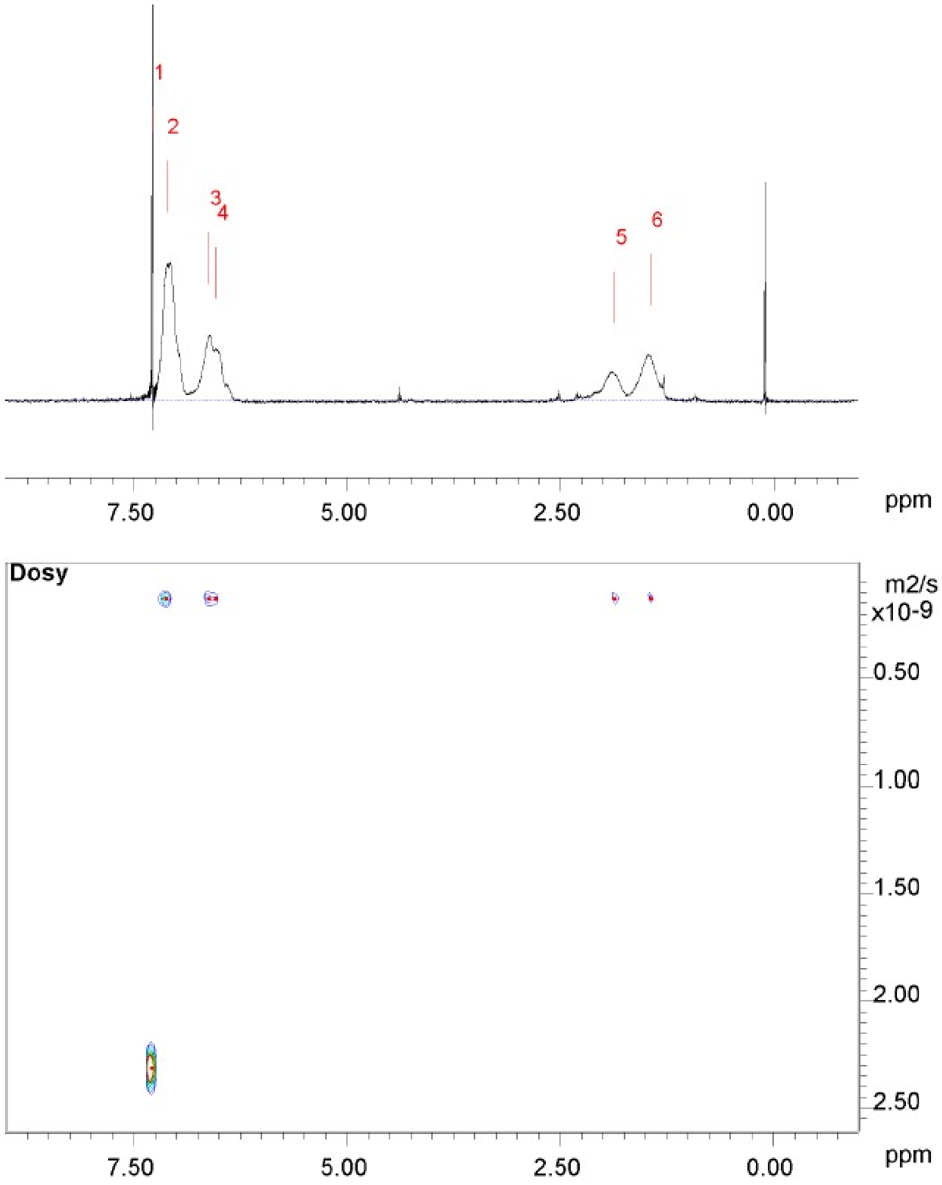

Peak name	F2 [ppm]	D [m2/s]	error
1	7.282	2.37e-09	5.131e-11
2	7.114	1.72e-10	1.255e-11
3	6.616	1.74e-10	1.291e-11
4	6.534	1.82e-10	1.358e-11
5	1.857	1.78e-10	2.082e-11
6	1.437	1.81e-10	1.496e-11

Figure S15. *DOSY report of* ***Cu$_2$-SCNPs****; measured in CDCl$_3$ (peak 1) at 298 K.*

DOSY report **Mo$_2$-SCNPs**:

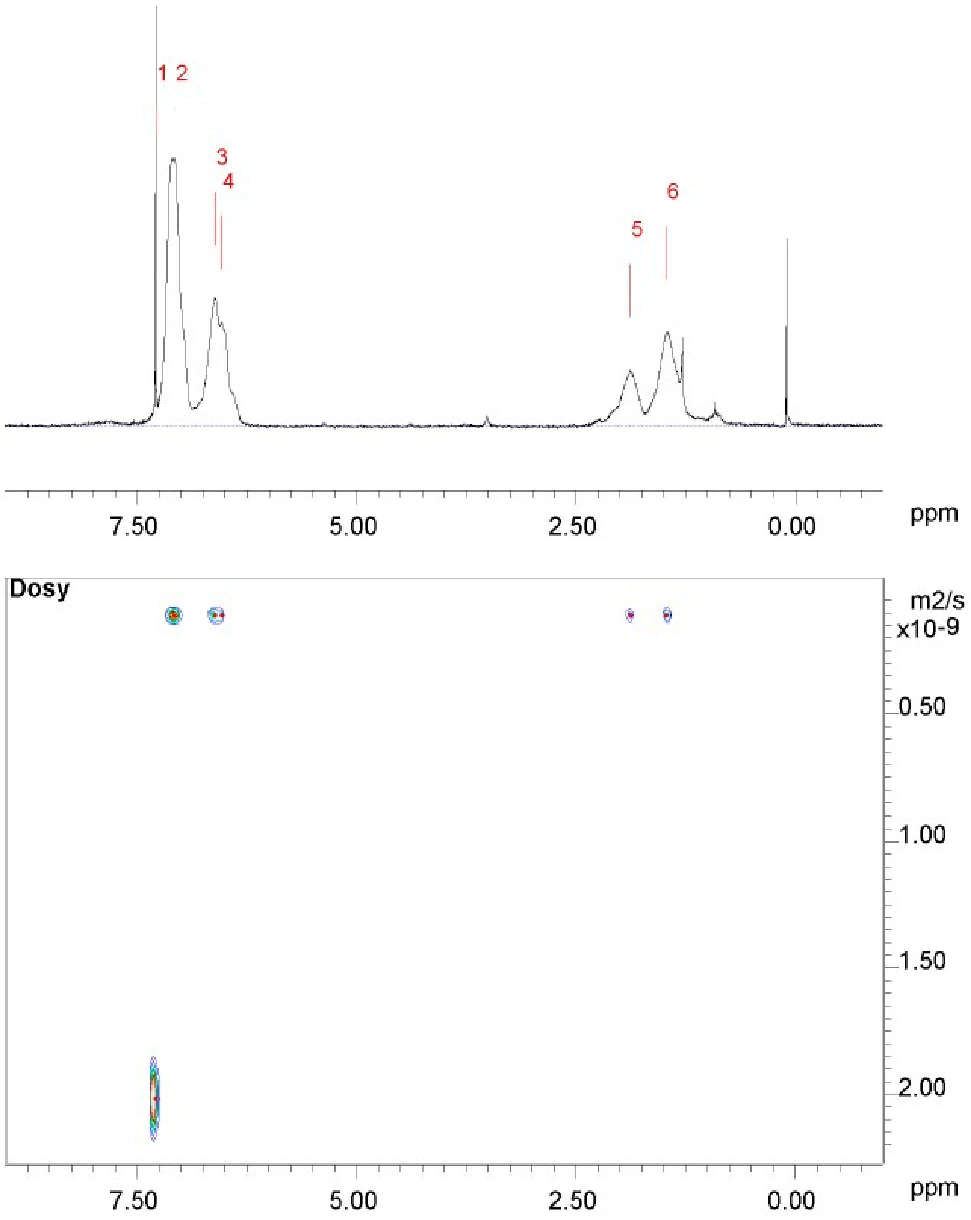

Peak name	F2 [ppm]	D [m2/s]	error
1	7.285	2.07e-09	7.152e-11
2	7.070	1.57e-10	8.647e-12
3	6.607	1.51e-10	9.834e-12
4	6.534	1.56e-10	8.786e-12
5	1.881	1.63e-10	1.120e-11
6	1.466	1.59e-10	7.923e-12

Figure S16. DOSY report of ***Mo$_2$-SCNPs****; measured in CDCl$_3$ (peak 1) at 298 K.*

IR Spectra

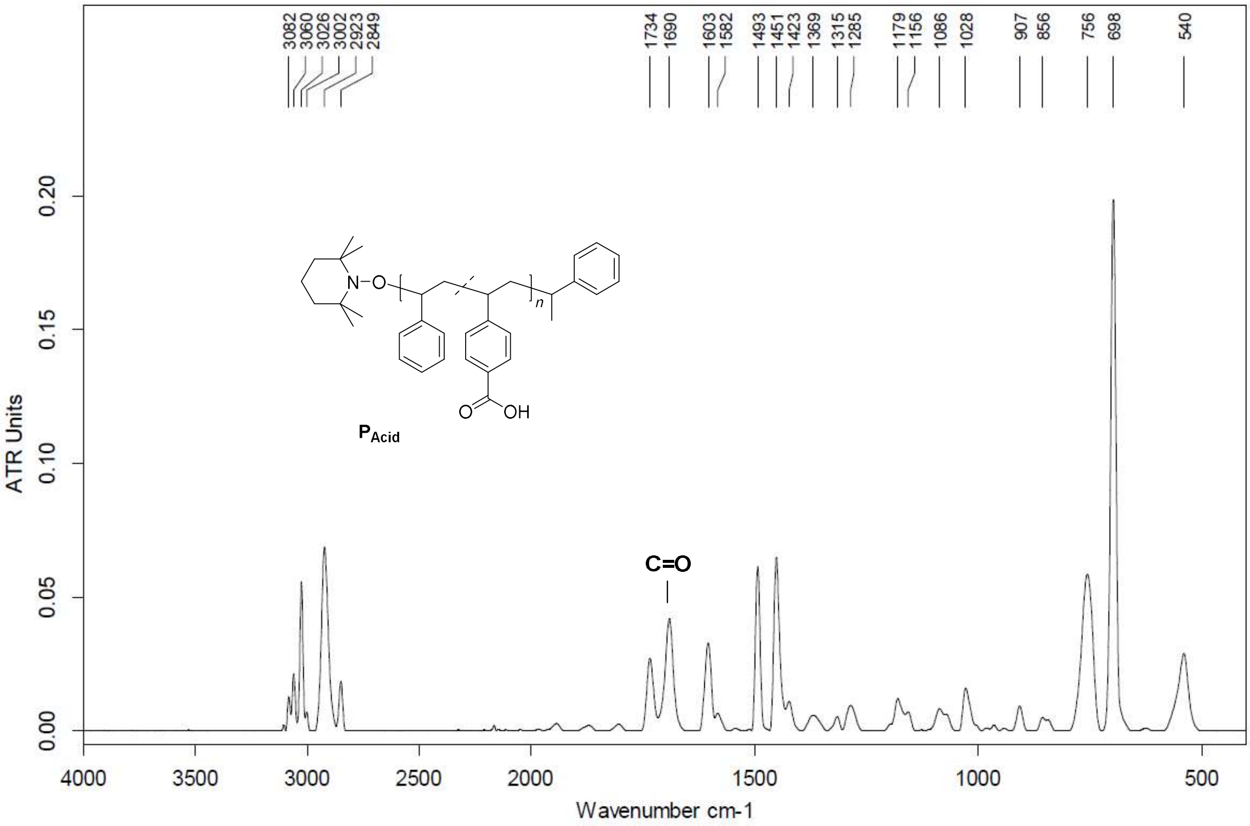

Figure S17. IR spectrum of copolymer P_{Acid}.

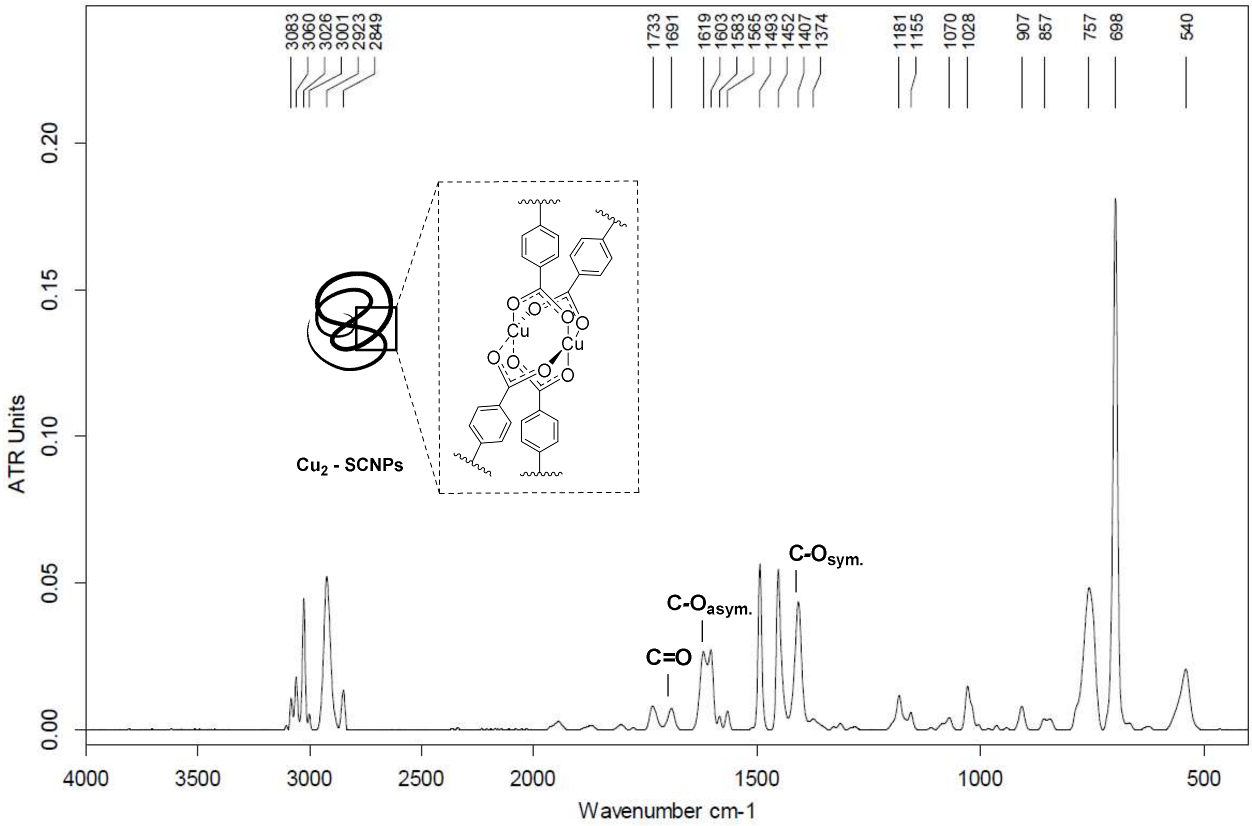

Figure S18. IR spectrum of ***Cu₂-SCNPs****.* The *C=O stretching mode of* ***P****$_{Acid}$ (Figure S17) has not disappeared completely, indicating free carboxylic acid moieties.*

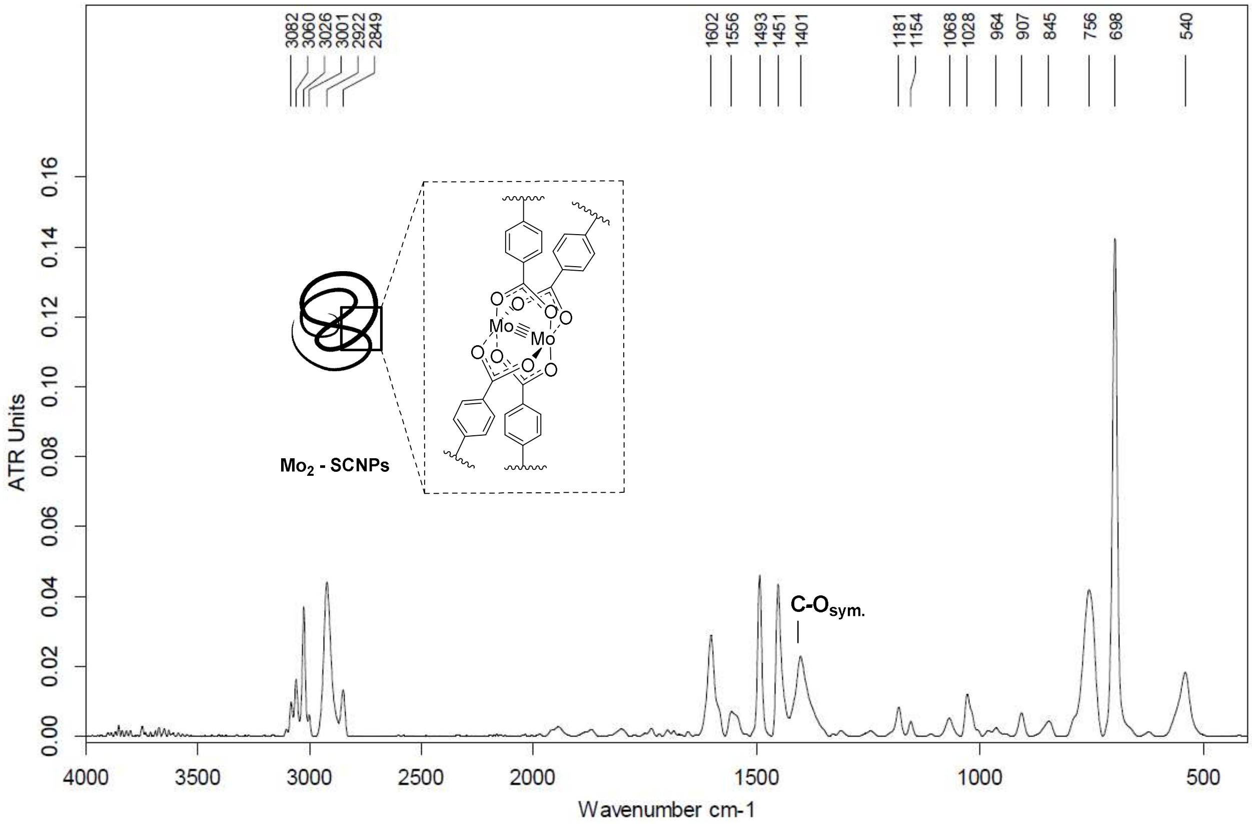

Figure S19. IR spectrum of ***Mo₂-SCNPs****. Due to overlaying bands, a band for the asymmetric C-O stretching mode cannot be observed.*

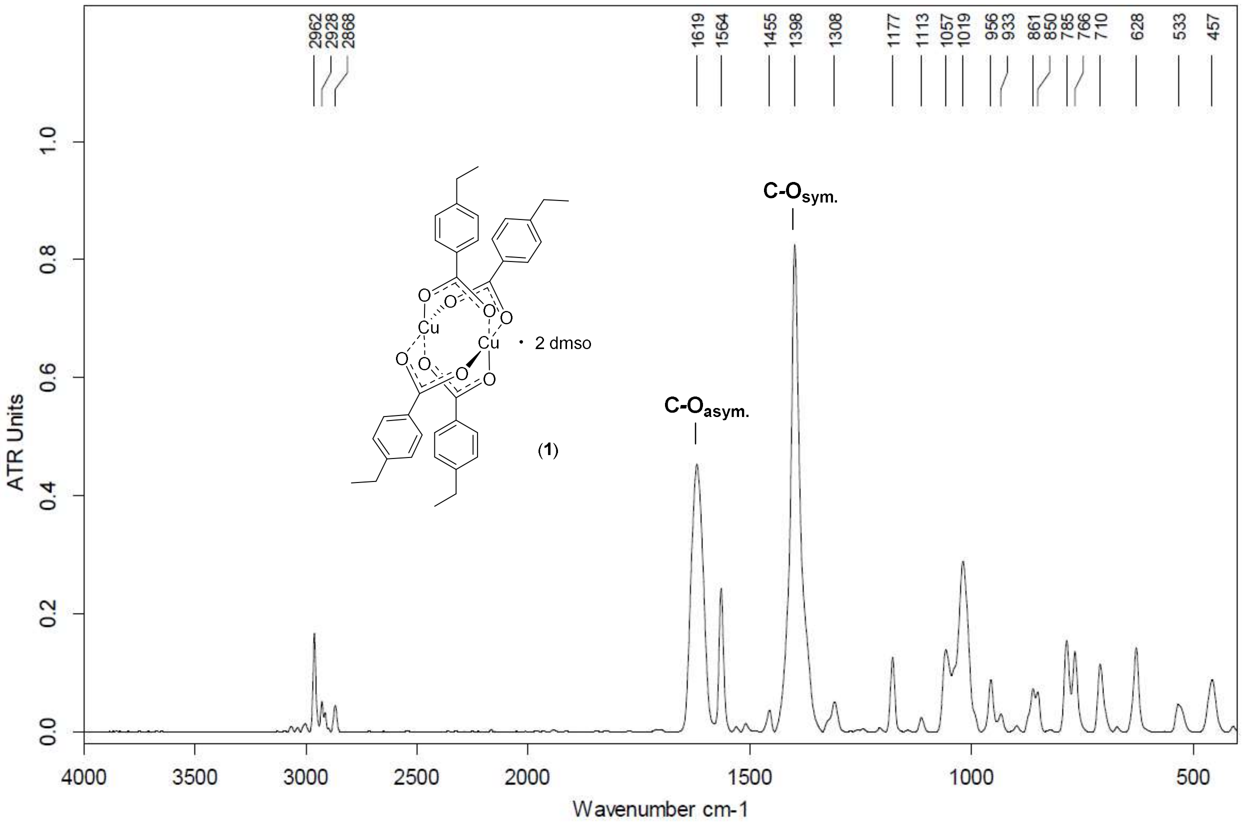

*Figure S20. IR spectrum of Cu_2-model compound **1**.*

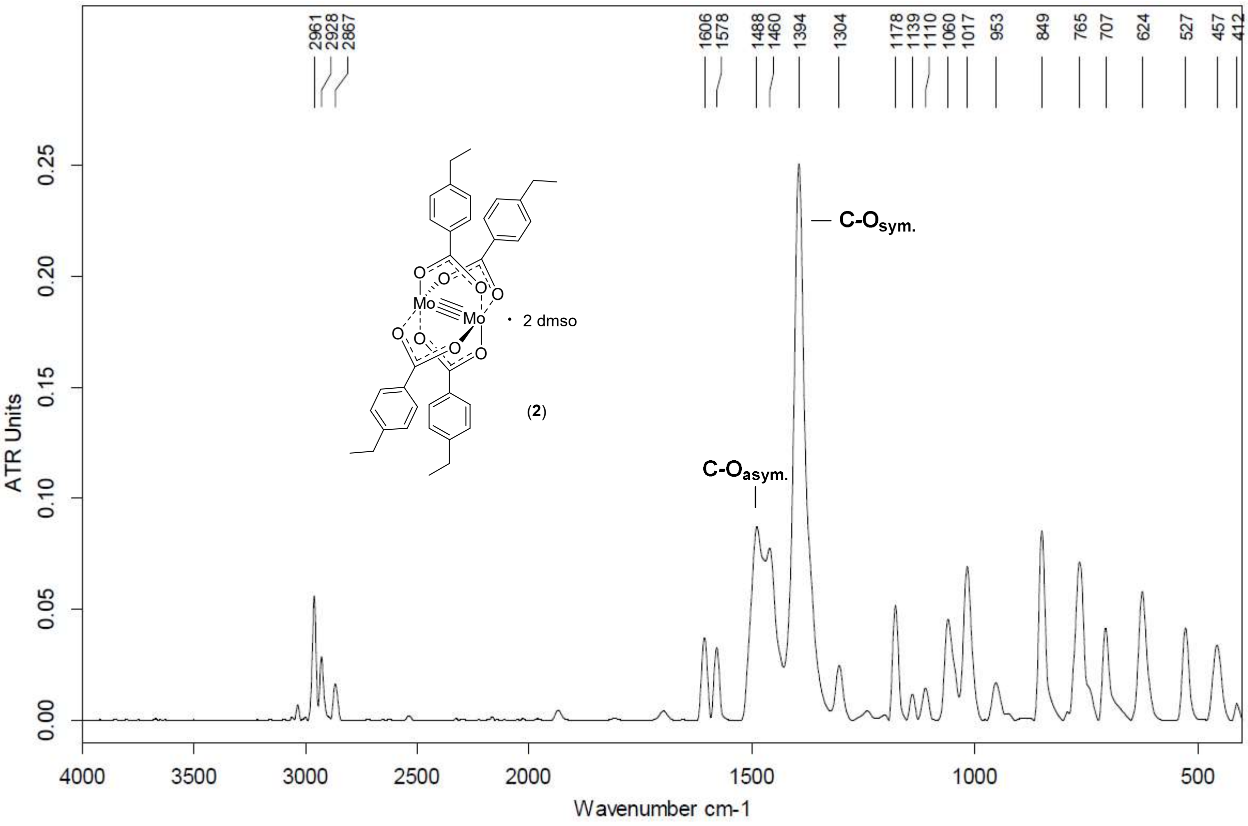

*Figure S21. IR spectrum of Mo_2-model compound **2**.*

Raman Spectra

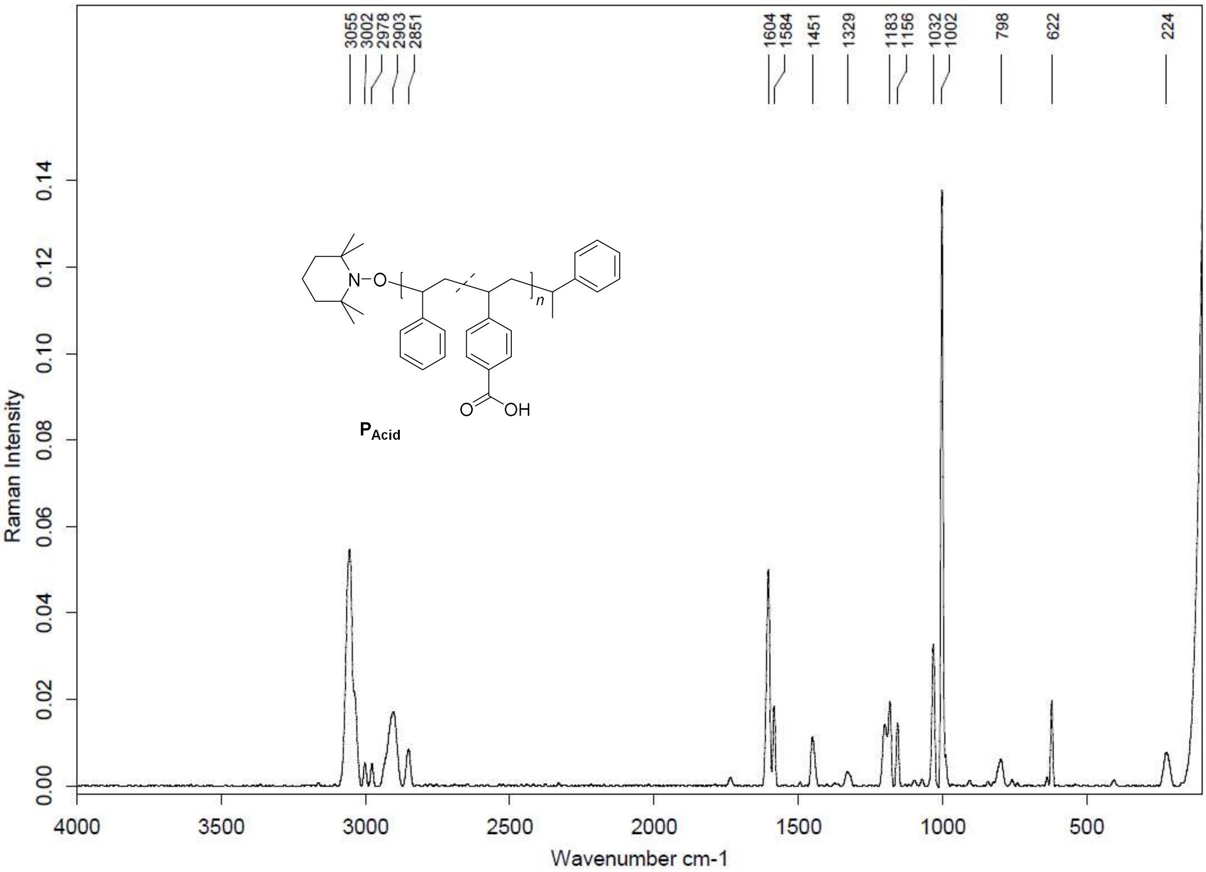

Figure S22. Raman spectrum of copolymer P_{Acid}.

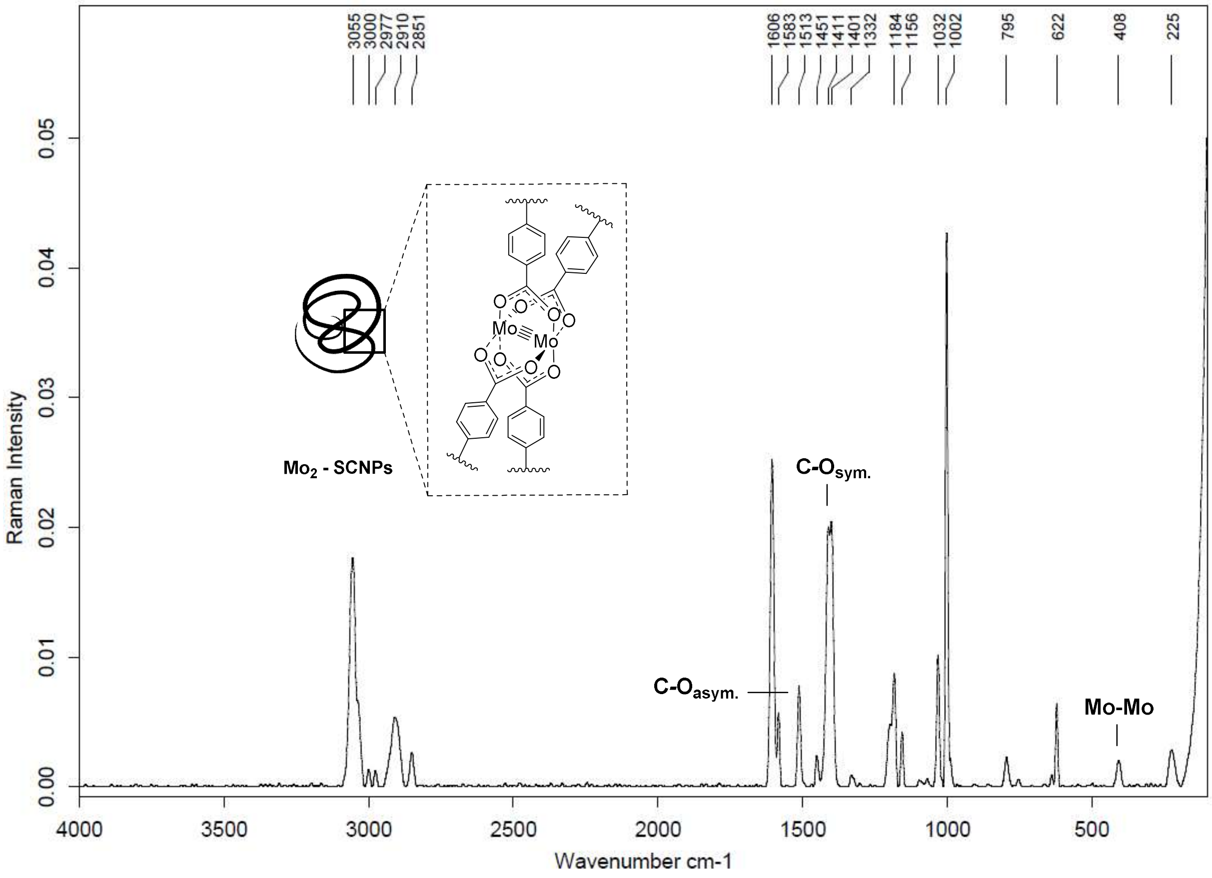

Figure S23. Raman spectrum of Mo_2-SCNPs.

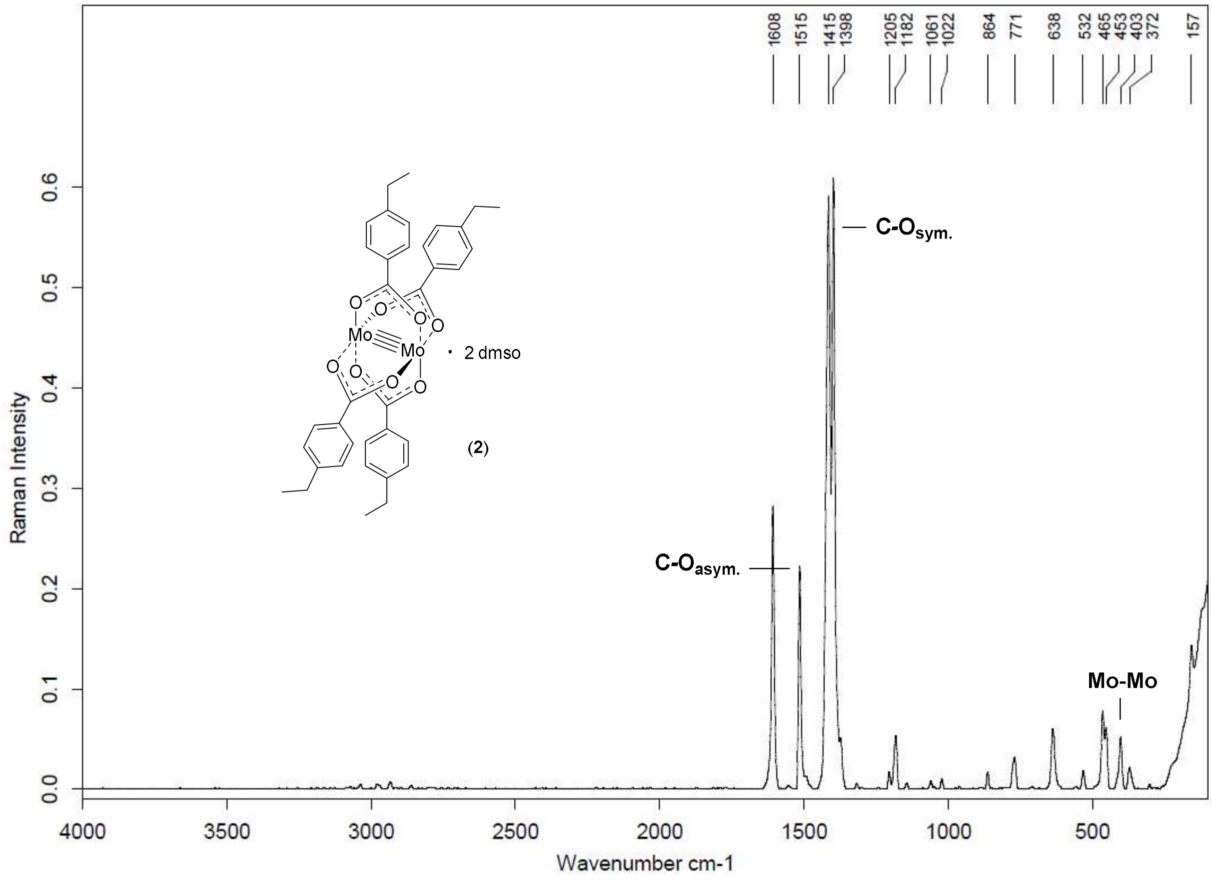

Figure S24. Raman spectrum of Mo_2-model compound 2.

UV-Vis Spectra

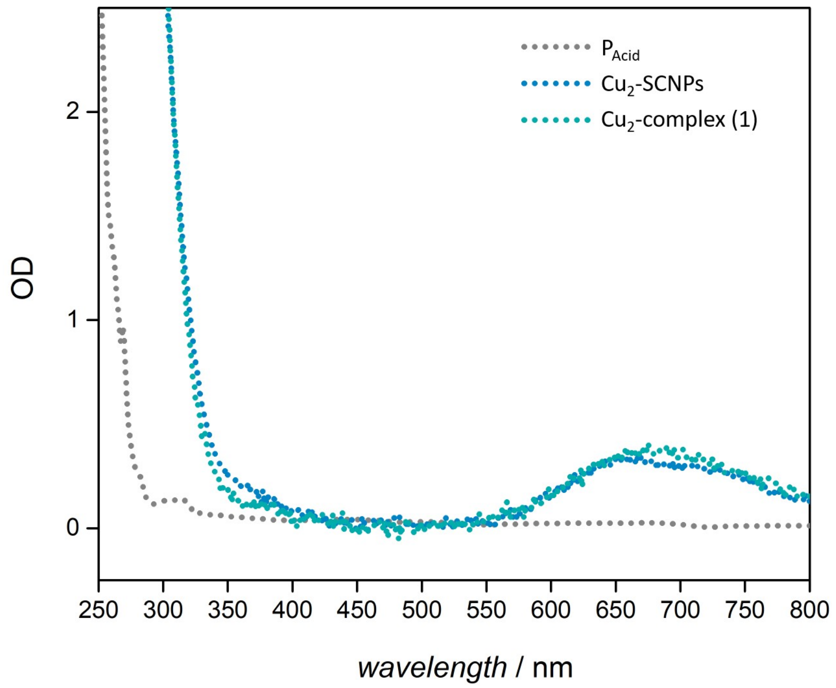

Figure S25. *UV-Vis spectra of* ***P_{Acid}, Cu_2-SCNPs*** *and the Cu_2-model complex* ***1***. *A broad absorption band between 550 – 800 nm is observed for the Cu_2 containing compounds.*

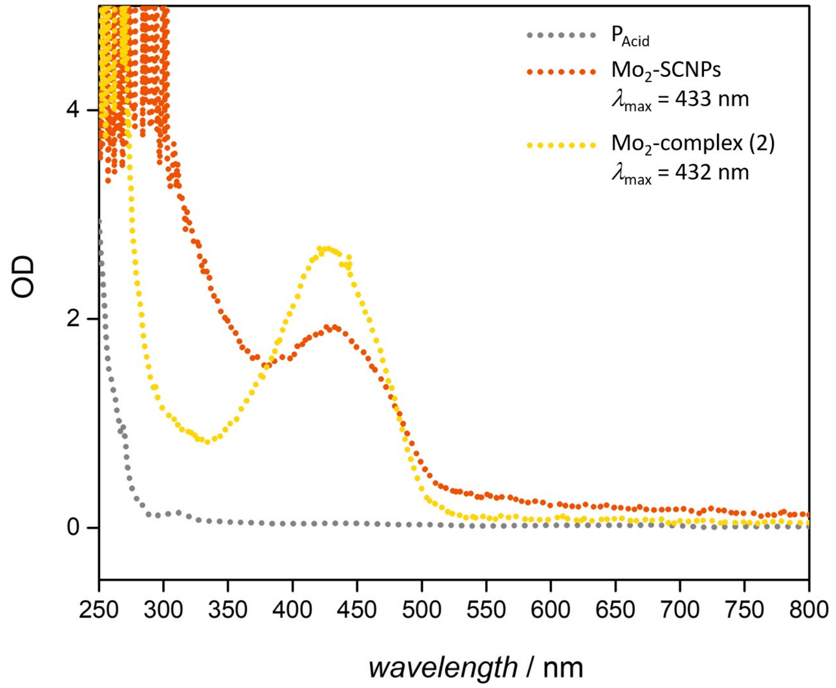

Figure S26. *UV-Vis spectra of* ***P_{Acid}, Mo_2-SCNPs*** *and the Mo_2-model complex* ***2***. *A local maximum absorbance at λ = 430 – 435 nm is observed for the Mo_2 containing compounds.*

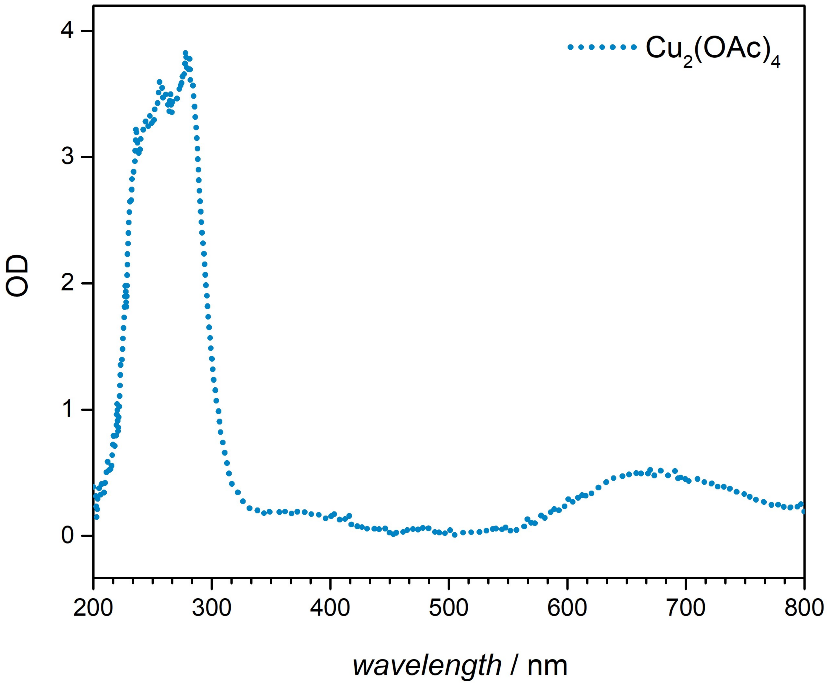

Figure S27. *UV-Vis spectrum of [Cu$_2$(OAc)$_4$].*

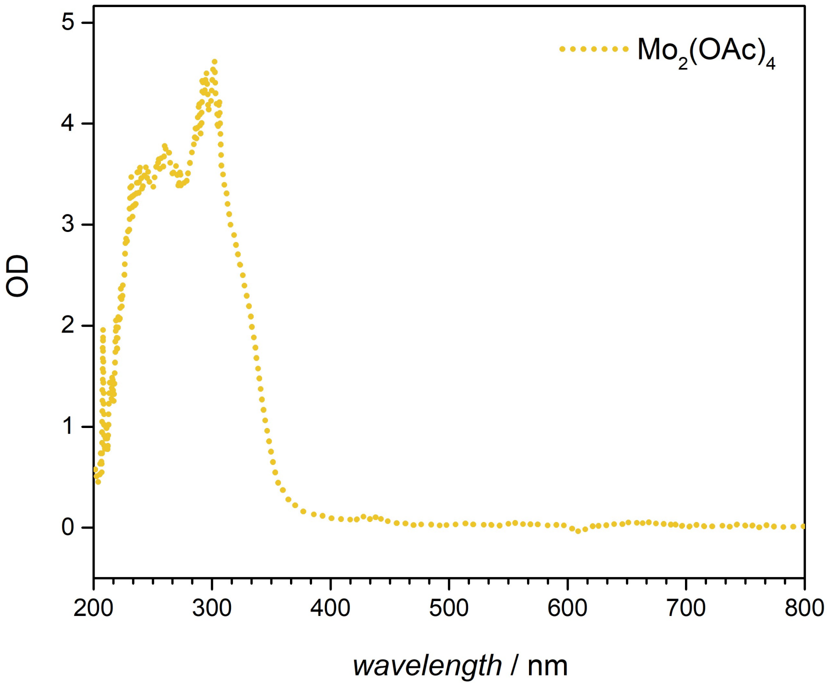

Figure S28. *UV-Vis spectrum of [Mo$_2$(OAc)$_4$].*

References

[1] T. A. Stephenson, E. Bannister, G. Wilkinson, *J. Chem. Soc.* **1964**, 2538-2541.

[2] N. D. Knöfel, H. Rothfuss, J. Willenbacher, C. Barner-Kowollik, P. W. Roesky, *Angew. Chem. Int. Ed.* **2017**, *56*, 4950-4954.

[3] A. C. Sunil, B. C. B. Bezuidenhoudt, J. M. Janse van Rensburg, *Acta Crystallogr. Sect. E* **2008**, *64*, m939.

[4] G. Sheldrick, *Acta Crystallogr. Sect. A* **2008**, *64*, 112-122.

[5] G. Sheldrick, *Acta Crystallogr. Sect. C* **2015**, *71*, 3-8.

[6] O. V. Dolomanov, L. J. Bourhis, R. J. Gildea, J. A. K. Howard, H. Puschmann, *J. Appl. Crystallogr.* **2009**, *42*, 339-341.

[7] D. R. Lide, *CRC Handbook of Chemistry and Physics, 85th Ed.*, Taylor & Francis, **2004**.